© 2021. Published by The Company of Biologists Ltd | Journal of Cell Science (2021) 134, jcs258419. doi:10.1242/jcs.258419

RESEARCH ARTICLE

A developmental stage- and Kidins220-dependent switch in astrocyte responsiveness to brain-derived neurotrophic factor

Fanny Jaudon[1,*,‡], Martina Albini[1,2,‡], Stefano Ferroni[3], Fabio Benfenati[1,4] and Fabrizia Cesca[1,5,§]

ABSTRACT

Astroglial cells are key to maintain nervous system homeostasis. Neurotrophins are known for their pleiotropic effects on neuronal physiology but also exert complex functions to glial cells. Here, we investigated (i) the signaling competence of mouse embryonic and postnatal primary cortical astrocytes exposed to brain-derived neurotrophic factor (BDNF) and, (ii) the role of kinase D-interacting substrate of 220 kDa (Kidins220), a transmembrane scaffold protein that mediates neurotrophin signaling in neurons. We found a shift from a kinase-based response in embryonic cells to a response predominantly relying on intracellular Ca^{2+} transients $[Ca^{2+}]_i$ within postnatal cultures, associated with a decrease in the synthesis of full-length BDNF receptor TrkB, with Kidins220 contributing to the BDNF-activated kinase and $[Ca^{2+}]_i$ pathways. Finally, Kidins220 participates in the homeostatic function of astrocytes by controlling the expression of the ATP-sensitive inward rectifier potassium channel 10 (Kir4.1) and the metabolic balance of embryonic astrocytes. Overall, our data contribute to the understanding of the complex role played by astrocytes within the central nervous system, and identify Kidins220 as a novel actor in the increasing number of pathologies characterized by astrocytic dysfunctions.

This article has an associated First Person interview with the first authors of the paper.

KEY WORDS: Kidins220, BDNF, Astrocytes, Ca^{2+} imaging, MAPK signaling, Lactate

INTRODUCTION

Astroglia, the most abundant cell population of the central nervous system (CNS), are taking the stage in the neuroscience field because of their multifaceted role in the modulation of neural physiology at increasing levels of complexity, i.e. from the single synapse to higher circuits (Santello et al., 2019). Key to astrocyte performance is the capability to sense a wide range of extracellular signals and, consequently, activate intracellular signaling pathways. These can be kinase-based – as the ubiquitous mitogen-activated protein kinase (MAPK), e.g. SHP2, Ras, ERK, pathways – or comprising signal transducer and activator of transcription 1 and 3 (STAT1 and STAT3), or nuclear factor kappa B (NFκB) cascades (Colombo and Farina, 2016), or initiated via second messengers that trigger the release of Ca^{2+} ions from the endoplasmic reticulum (Okubo, 2020). Intracellular Ca^{2+} transients ($[Ca^{2+}]_i$) underlie the vast majority of responses of astrocytes as they mediate the release of a plethora of soluble factors, i.e. gliotransmitters, that include neurotransmitters, trophic factors, hormones, cytokines and several other bio-active molecules. Gliotransmitters exert both autocrine and paracrine functions, thus controlling and coordinating the activity of astroglia and of neighboring neurons (Verkhratsky et al., 2016).

Although the mechanisms that underlie astrocyte uptake/release of glutamate, ATP and other gliotransmitters – as well as the ability to respond to neurotransmitters, such as glutamate – have been well-described and agreed upon by the scientific community, the extent to which astrocytes produce, sense and respond to neurotrophins, such as nerve-growth factor (NGF) and brain-derived neurotrophic factor (BDNF), is still an object of debate. Neurotrophins are mostly studied for their pleiotropic effects on neurons, as they control virtually every aspect of neuronal physiology, including maturation, axonal and dendritic differentiation, synaptogenesis and various forms of synaptic plasticity (Park and Poo, 2013). Besides their well-known effects on neurons, neurotrophins also modulate important aspects of astrocyte physiology (Poyhonen et al., 2019). Within the CNS, the most abundant neurotrophin is BDNF, which signals through its full-length receptor, the neurotrophic receptor tyrosine kinase 2 (TrkB, also known as NTRK2), or the kinase-deficient truncated version of it (TrkB-T1) (Park and Poo, 2013). Astrocytes predominantly express TrkB-T1, which triggers release of Ca^{2+} from intracellular stores (Rose et al., 2003) and activates various kinase pathways (Ohira et al., 2005; Vaz et al., 2011) independently of the full-length protein. The BDNF-TrkB-T1 system modulates several astrocyte properties, such as astrocyte morphological maturation, and their capability of sensing neurotransmission by controlling the membrane targeting of glycine and GABA transporters (Aroeira et al., 2015; Holt et al., 2019; Ohira et al., 2007; Vaz et al., 2011). An aberrant activation of this pathway has been described in the experimental autoimmune encephalomyelitis rodent model for multiple sclerosis, where overexpressed TrkB-T1 induces neuronal death by promoting the release of nitric oxide (Colombo et al., 2012). Moreover, astrocytic TrkB-T1 contributes to neuropathic pain and neurological dysfunctions in rodent models of spinal cord injury and of amyotrophic lateral sclerosis (Matyas et al., 2017; Yanpallewar et al., 2021). TrkB-T1 is, arguably, the predominant receptor isoform expressed in astrocytes; however, some reports have indicated that cultured astrocytes can also express full-length TrkB (Climent et al., 2000; Condorelli et al., 1995). Interestingly, some evidence indicates that TrkB expression by astrocytes occurs upon injury of the CNS or in the presence of chronic and

[1]Center for Synaptic Neuroscience and Technology, Istituto Italiano di Tecnologia, 16132 Genova, Italy. [2]Department of Experimental Medicine, University of Genova, 16132 Genova, Italy. [3]Department of Pharmacy and Biotechnology, University of Bologna, 40126 Bologna, Italy. [4]IRCCS Ospedale Policlinico San Martino, 16132 Genova, Italy. [5]Department of Life Sciences, University of Trieste, 34127 Trieste, Italy.
*Present address: Department of Life Sciences, University of Trieste, 34127 Trieste, Italy.
‡These authors contributed equally to this work

§Author for correspondence (fcesca@units.it)

F.C., 0000-0003-2190-6314

Handling Editor: Giampietro Schiavo
Received 16 January 2021; Accepted 12 July 2021

Journal of Cell Science (2021) 134, jcs258419. doi:10.1242/jcs.258419

inflammatory diseases, such as multiple sclerosis (McKeon et al., 1997; Soontornniyomkij et al., 1998; Stadelmann et al., 2002). Importantly, the competence of astrocytes to perceive and respond to BDNF seems to be different in various brain areas (Saba et al., 2020), thus adding a further layer of complexity to the system. Besides sensing extracellular BDNF through specific receptors, astrocytes also take up and recycle BDNF as well as its precursor form (proBDNF) *in vitro* and *in vivo* (Bergami et al., 2008; Vignoli et al., 2016). An increasing body of evidence suggests that cultured astrocytes produce and secrete BDNF under basal conditions (Kinboshi et al., 2017; Rousseaud et al., 2015), and that BDNF expression is increased by specific stimuli (Inoue et al., 1997; Jean et al., 2008; Miklic et al., 2004; Saha et al., 2006; Zafra et al., 1992). Albeit less studied than the BDNF-TrkB system, astrocytes also express the tumor necrosis factor receptor superfamily member 16 (NGFR, hereafter referred to as $p75^{NTR}$), which binds all pro-neurotrophins that mediate distinct signaling pathways with similar affinity. Astrocytes upregulate $p75^{NTR}$ upon injuries or cellular insults, and astrocytic $p75^{NTR}$ has been involved in the modulation of cell proliferation associated with astrocytosis and the formation of glial scars (reviewed by Cragnolini and Friedman, 2008).

Although the contribution of astrocytes to neuronal function is becoming clear, the cellular and molecular mechanisms that underlie the regulation of communication between astrocytes and neurons mediated by neurotrophins remains incompletely understood. Kinase D-interacting substrate of 220 kDa (Kidins220) is one of the several proteins involved in the neurotrophin pathways. Kidins220 is a four-pass transmembrane protein enriched in the nervous system, where it is expressed by both neurons and astrocytes, and involved in various aspects of neuronal differentiation and plasticity (Neubrand et al., 2012; Scholz-Starke and Cesca, 2016). Recently, we have shown that Kidins220 participates in the molecular events that induce spontaneous and evoked $[Ca^{2+}]_i$ transients in primary astrocytes, thereby controlling the vulnerability of astrocytes to genotoxic stress and the maturation of co-cultured neurons (Jaudon et al., 2020).

In this work, we investigated the responsivity of astrocytes to BDNF and the role of Kidins220 in astrocytic BDNF signaling. We first compared the signaling competence of embryonic and postnatal primary cortical astrocytes exposed to BDNF, and found a developmental shift from a kinase-based response in embryonic cells to a predominantly $[Ca^{2+}]_i$-based response in postnatal cultures, which was paralleled by the reduced expression of full-length TrkB. We also addressed the role of Kidins220 in BDNF-induced signaling within astrocytes, and found that Kidins220 significantly contributes to both kinase and $[Ca^{2+}]_i$ pathways. Our data contribute to the understanding of the complex astrocytic response to neurotrophins, describing a developmental stage- and Kidins220-dependent switch in the responsiveness of astrocytes to BDNF.

RESULTS

BDNF induces activation of intracellular signaling pathways mediated by full-length TrkB and Kidins220 in embryonic astrocytes

To determine the role of Kidins220 in the modulation of BDNF signaling in astrocytes, we compared expression of TrkB in wild-type (+/+) and Kidins220$^{-/-}$ primary astrocytes by using western blot analysis. Astrocytes were derived from E18.5 embryos and used after 15 days *in vitro* (DIV), a stage at which cultures had reached confluence. Compared with wild-type cells, Kidins220$^{-/-}$ astrocytes displayed a significant reduction of both full-length and truncated TrkB forms (~40% and 50%, respectively), although the ratio between these two isoforms remained unchanged (Fig. 1A). In contrast, no differences were detected in the expression of $p75^{NTR}$ in the two genotypes (Fig. S1A). We then compared expression levels of the main downstream effectors of the BDNF-TrkB pathway, i.e. of mitogen-activated protein kinases 1 and 2 (MAPK1 and 2), phospholipase C-gamma-1 (PLCG1, hereafter referred to as PLCγ) and Akt. Whereas total protein levels of MAPK1/2 and Akt1, 2 and 3 (hereafter referred to as Akt) were unaffected, we found a significant reduction of PLCγ in Kidins220$^{-/-}$ astrocytes (Fig. 1B). We then asked whether ablation of Kidins220 in these cells affects the response to BDNF and TrkB-mediated signaling. At 15 DIV, astrocytes were treated with 50 ng/ml BDNF for 5 or 30 min and levels of phosphorylated forms of MAPK1/2, PLCγ and Akt (P-MAPK, P-PLCγ and P-Akt, respectively) were quantified by western blotting using phospho-specific antibodies (Fig. 1C). Whereas basal levels of phosphorylated MAPK1/2 and Akt were unchanged in Kidins220$^{-/-}$ astrocytes, we observed a reduction upon BDNF stimulation that reached statistical significance for MAPK1/2 at 30 min. Prolonged treatment with BDNF (up to 2 h) did not further increase levels of P-MAPK and P-Akt in wild-type or Kidins220$^{-/-}$ astrocytes; moreover, in knock-out (KO) samples, levels of P-MAPK and P-Akt dropped to even lower levels compared with those in wild-type cells exposed to BDNF for 2 h (Fig. S2A). This indicates that absence of Kidins220 affects the magnitude of the BDNF response and not its kinetics. We also detected a significant reduction of the basal PLCγ phosphorylation levels, whereas the percent increase in PLCγ phosphorylation induced by the BDNF was similar in wild-type and Kidins220$^{-/-}$ astrocytes. A similar trend was observed when BDNF was used at lower concentration (1 ng/ml). However, in this case, the fold increase of MAPK phosphorylation was reduced compared to that when 50 ng/ml BDNF were used for stimulation (Fig. S2B). Of note, we were unable to detect reliable phosphorylation of PLCγ under these experimental conditions (not shown). Whereas astrocytes predominantly express TrkB-T1, there has been some indication that primary astrocytes also express full-length neurotrophin receptors under physiological conditions and/or upon specific stimuli (Climent et al., 2000; Condorelli et al., 1994; Hutton et al., 1992). Although, under our culturing conditions, primary glial cultures are predominantly represented by astrocytes – with only a small percentage of microglial cells (Jaudon et al., 2020), we wanted to confirm that the observed activation of signaling pathways is, indeed, ascribable to astrocytes. Thus, we performed immunostaining experiments using antibodies specifically recognizing TrkB phosphorylated at Tyr516, i.e. the site required to be phosphorylated to activate MAPK, as well as antibodies against GFAP. Indeed, stimulation with BDNF increased fluorescence intensity of pTrkB in GFAP-positive cells, confirming that full-length TrkB activation occurred in astrocytes (Fig. 1D).

Together these results show that, similar to its function in neurons (Arevalo et al., 2004; Cesca et al., 2012), Kidins220 is a crucial regulator of BDNF-dependent TrkB signaling also in astrocytes.

Expression of full-length TrkB and activation of BDNF-dependent kinase pathways are reduced in postnatal wild-type astrocytes

Astrocytes undergo important physiological changes from the embryonic development to the postnatal period, accompanied by variations in the expression pattern of several signaling proteins (Dallerac et al., 2018). To study the developmental changes associated with the BDNF-TrkB system, we prepared primary astrocyte cultures using P0-P1 mouse pups derived by crossing

Journal of Cell Science (2021) 134, jcs258419. doi:10.1242/jcs.258419

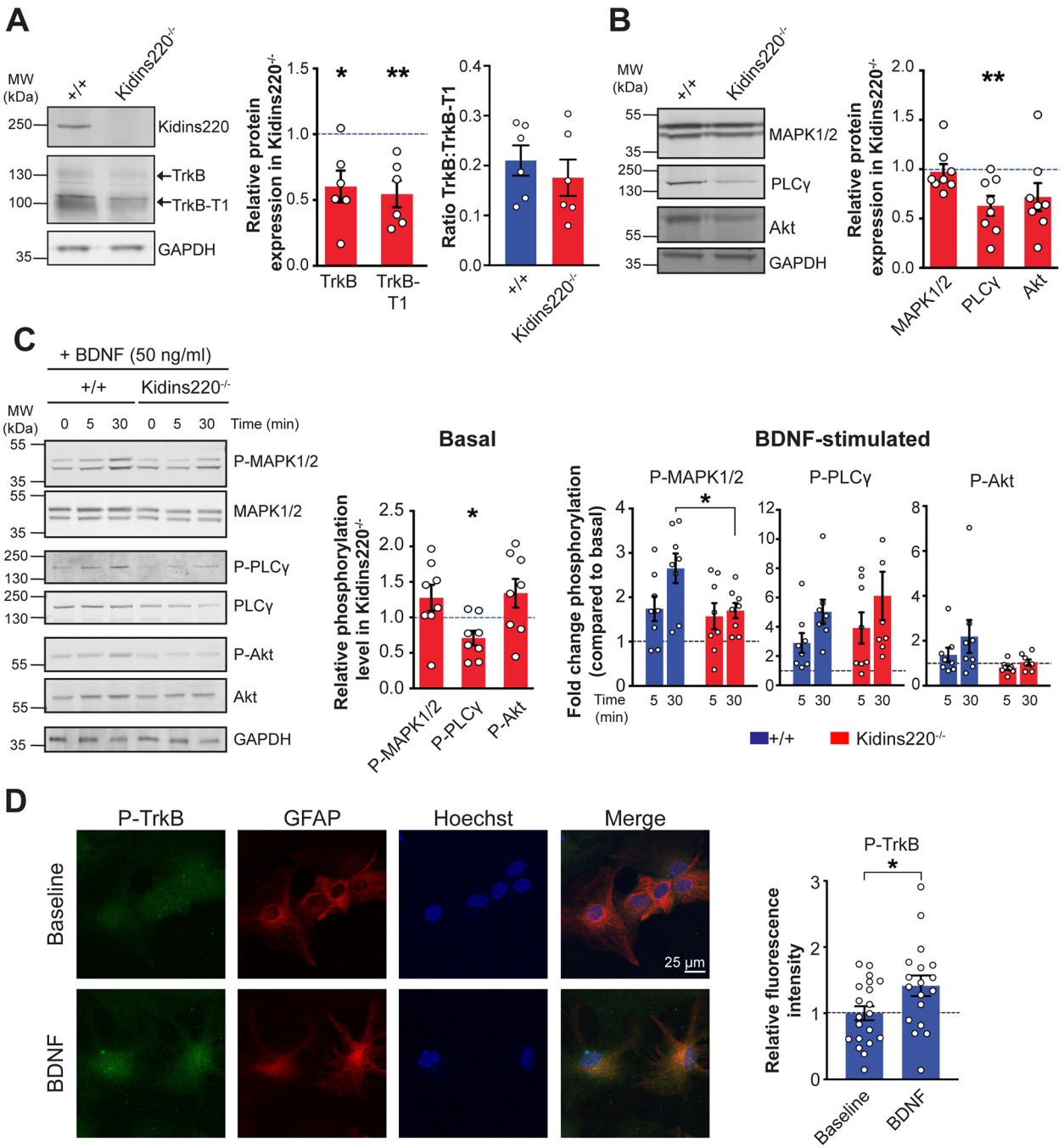

Fig. 1. TrkB-dependent BDNF signaling is impaired in Kidins220$^{-/-}$ embryonic astrocytes. (A,B) Protein extracts from wild-type (+/+) and Kidins220$^{-/-}$ embryonic astrocyte cultures after 15 DIV were analyzed by western blotting using anti-Kidins220 and anti-TrkB antibodies (A); anti-MAPK1/2, anti-PLCγ and anti-Akt antibodies (B). Representative immunoblots are shown on the left; a quantification of immunoreactive bands is plotted on the right. The intensity of bands from Kidins220$^{-/-}$ samples was normalized to that of corresponding wild-type samples within the same nitrocellulose membrane. *P<0.05, **P<0.01, one sample Student's t-test; wild-type and Kidins220$^{-/-}$ cultures were n=6 (A) and n=8 (B). (C) Wild-type and Kidins220$^{-/-}$ astrocyte cultures were treated with 50 ng/ml BDNF for 5 and 30 min or left untreated (0). Lysates were analyzed for phosphorylated MAPK1/2 (Thr202/Tyr204; P-MAPK1/2), PLCγ (Tyr783; P-PLCγ) and Akt (Ser473; P-Akt). Membranes were subsequently stripped and re-probed for the total amount of the same protein. Representative immunoblots are shown on the left. Phosphorylation of MAPK1/2, PLCγ and Akt in lysates of untreated wild-type and Kidins220$^{-/-}$ cells (basal levels) are plotted in the middle graph. Data were analyzed as described for A and B. Time dependence of MAPK1/2, PLCγ and Akt phosphorylation upon stimulation with BDNF of wild-type and Kidins220$^{-/-}$ astrocytes is plotted on the right. Graphs show the fold-change of MAPK1/2, PLCγ and Akt activation compared to phosphorylation levels in untreated samples for each genotype, set to 1 (dashed line in all graphs). The fold-change activation was calculated as follows: we first calculated the phospho:total intensity ratio for each sample, and subsequently divided the phospho:total ratio of every treated sample by the phospho:total ratio of the untreated (control) sample within the same membrane. For MAPK, we calculated the sum of MAPK1 and MAPK2 immunoreactivity. *P<0.05, unpaired Student's t-test, n=8 for both wild-type and Kidins220$^{-/-}$ cultures. For all experiments, GAPDH was used as a loading control. (D) Left: Representative confocal images of wild-type astrocytes treated with BDNF (1 ng/ml for 5 min) or not treated, stained with anti-pTrkB (Tyr516, green) and anti-GFAP (red) antibodies, and Hoechst to visualize nuclei. Scale bar: 25 µm. Right: Quantification of pTrkB fluorescence intensity in GFAP-positive cells. *P<0.05, unpaired Student's t-test, n=20 (not treated) and 18 (BDNF-treated) cells from three independent preparations. Data show the average pTrkB fluorescence intensity of all GFAP-positive cells within each field. Values are expressed as the means±s.e.m.

Journal of Cell Science

Journal of Cell Science (2021) 134, jcs258419. doi:10.1242/jcs.258419

Kidins220$^{+/lox}$ with Kidins220$^{+/lox}$ mice, which allowed us to have both wild-type and Kidins220$^{lox/lox}$ animals in the same litter. We chose this strategy since the full knockout of Kidins220 causes embryonic lethality, thus precluding the possibility of performing postnatal dissection (Cesca et al., 2011, 2012). We first compared the expression levels of full-length and truncated TrkB receptors in wild-type embryonic and postnatal preparations, and found a specific reduction of the full-length isoform in postnatal cultures. This led to a decrease in the ratio of TrkB:TrkB-T1 compared with that in embryonic cells (Fig. 2A). In contrast, expression of p75^{NTR} was comparable in embryonic and postnatal wild-type cells (Fig. S1B). Wild-type postnatal cultures exposed to 50 ng/ml BDNF showed an appreciable increase of phosphorylated Akt and MAPK1/2, although the fold-increase of P-MAPK1/2 was less than that observed in embryonic cultures (1.2-fold versus 2.5-fold at 30 min; compare Figs 2B and 1C), probably a consequence of reduced TrkB expression. Similar results were observed with a lower BDNF concentration (1 ng/ml; Fig. S3).

Kidins220 controls expression of both TrkB and TrkB-T1 but is dispensable for activation of BDNF-dependent kinase pathways in postnatal astrocytes

Primary Kidins220$^{lox/lox}$ cultures were infected with lentiviruses expressing either the active form of Cre recombinase to induce depletion of Kidins220 or a functionally inactive form of Cre (ΔCre) as control (Kaeser et al., 2011; see Materials and Methods for details). We refer to these cultures as Kidins220-depleted (Kidins220$^{lox/lox\text{-}Cre}$) and control (Kidins220$^{lox/lox\text{-}\Delta Cre}$) cultures. Although Cre-induced depletion of Kidins220 in postnatal preparations yielded reduced levels of full-length and truncated TrkB, the TrkB to TrkB-T1 ratio remained unaltered (Fig. 3A). Levels of p75^{NTR} were also unchanged in the absence of Kidins220 (Fig. S1C). Both results are in full agreement with those obtained on embryonic cultures. We then analyzed the signaling capability of postnatal cultures in the presence or absence of Kidins220. The basal expression levels of MAPK1/2, PLCγ and Akt were not affected by depletion of Kidins220 (Fig. 3B). Moreover, in contrast to the data obtained in embryonic cultures, removal of Kidins220 in postnatal cultures did not affect activation of BDNF-induced phosphorylation of MAPK1/2, PLCγ and Akt (Fig. 3C and Fig. S4).

Altogether, the data presented in Figs 2 and 3 show (i) reduced protein levels of full-length TrkB and reduced activation of kinase pathways upon exposure to BDNF in wild-type postnatal astrocytes compared to embryonic cells; and (ii) a further reduction of both TrkB and TrkB-T1 levels in the absence of Kidins220. However the limited activation of kinase pathways induced by BDNF was not impacted upon depletion of Kidins220.

Depletion of Kidins220 impairs BDNF-induced $[Ca^{2+}]_i$ transients in postnatal astrocytes

We subsequently investigated the role played by Kidins220 in BDNF-induced $[Ca^{2+}]_i$ signaling by monitoring BDNF-induced $[Ca^{2+}]_i$ transients in astrocytes (Rose et al., 2003). In embryonic cultures, very few cells responded to BDNF stimulation – 9.8% for wild-type and 7.4% for Kidins220$^{-/-}$ (Fig. 4A) and responsive cells displayed modest $[Ca^{2+}]_i$ variations (Fig. 4B,C). In contrast, ∼30–35% of cells in postnatal cultures responded with sizable $[Ca^{2+}]_i$ peaks to BDNF (Fig. 4D–F). Whereas the percentage of responding cells was not affected by Kidins220 depletion (Fig. 4D), the average amplitude of BDNF-induced $[Ca^{2+}]_i$ transients was significantly reduced in absence of Kidins220 (Fig. 4E and F; $^{\#}P$=0.0432 genotype effect). To investigate the contribution of the different isoforms of TrkB in this process, we repeated the same experiments in the presence of either the tyrosine kinase blocker K-252a (Cesca et al., 2012) to specifically inhibit the full-length TrkB isoform, or the TrkB antagonist ANA-12 (Cazorla et al., 2011) to block both TrkB and TrkB-T1. Pre-incubation of cells with K-252a did not affect the percentage of BDNF-responding cells (Fig. 4D, bars on shaded background). However, the amplitude of the

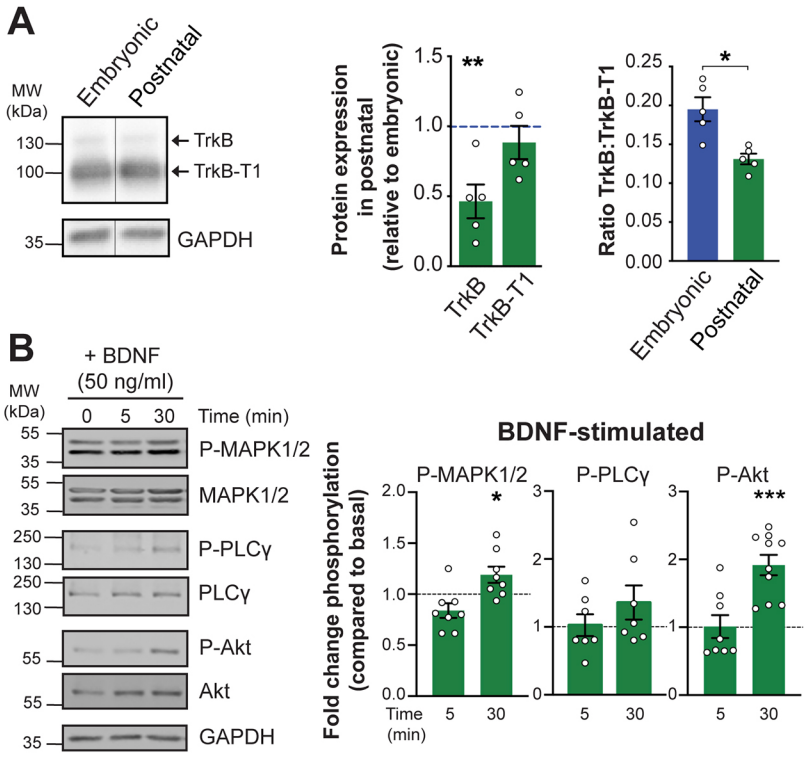

Fig. 2. Expression of full-length TrkB is reduced in postnatal astrocytes. (A) Protein extracts from wild-type embryonic and postnatal cultures were analyzed by western blotting with anti-TrkB antibodies. A representative immunoblot is shown on the left; quantification of immunoreactive bands is plotted on the right. Intensity of bands from postnatal samples was normalized to the corresponding bands from wild-type embryonic samples within the same nitrocellulose membrane. *P<0.05, **P<0.01, one sample Student's t-test, n=5 wild-type embryonic and postnatal cultures. (B) Postnatal wild-type astrocyte cultures were treated with 50 ng/ml BDNF for 5 or 30 min, or left untreated (0). Lysates were analyzed for phosphorylated MAPK1/2 (Thr202/Tyr204; P-MAPK1/2), Akt (Ser473; P-Akt) and PLCγ (Tyr783; P-PLCγ). Membranes were subsequently stripped and re-probed for the total amount of the same protein. Representative immunoblots are shown of the left. Time dependence of MAPK1/2, PLCγ and Akt phosphorylation in response to BDNF in wild-type postnatal astrocytes is shown on the right. Graphs express the fold-change of MAPK1/2, PLCγ and Akt activation compared to phosphorylation levels in untreated samples, set to 1 (dashed line in all graphs). The fold-change of activation was calculated as described in Fig. 1. For MAPK, we report the sum of MAPK1 and MAPK2 immunoreactivity. *P<0.05, ***P<0.001, one sample Student's t-test compared to baseline, n=7–8 independent cultures. Values are expressed as the means±s.e.m. in all panels.

Journal of Cell Science (2021) 134, jcs258419. doi:10.1242/jcs.258419

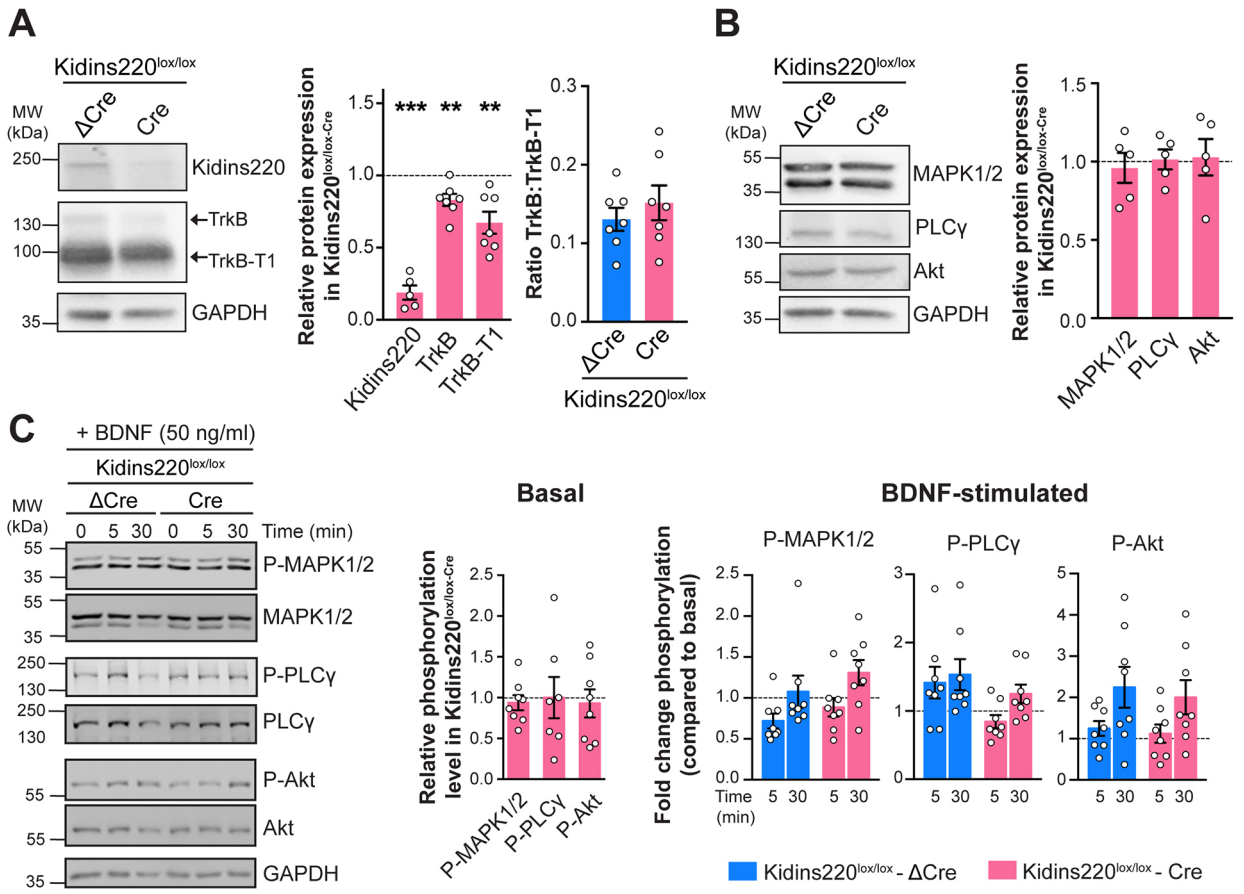

Fig. 3. Removal of Kidins220 in postnatal astrocyte cultures does not alter TrkB-dependent BDNF signaling. (A,B) Protein extracts from Kidins220$^{lox/lox}$ P0-P1 astrocyte cultures infected with lentiviruses encoding catalytically dead (ΔCre) or active Cre recombinase were analyzed by western blotting using anti-Kidins220 and anti-TrkB antibodies (A), and anti-MAPK1/2, anti-PLCγ and anti-Akt antibodies (B). Representative immunoblots are shown on the left; quantification of immunoreactive bands is plotted on the right. The intensity of bands from Kidins220$^{lox/lox\text{-}Cre}$ samples was normalized to the corresponding bands from Kidins220$^{lox/lox\text{-}\Delta Cre}$ samples within the same nitrocellulose membrane. ***P*<0.01, ****P*<0.001, one sample Student's *t*-test, *n*=5-7 Kidins220$^{lox/lox}$ cultures. (C) Kidins220$^{lox/lox\text{-}Cre}$ and Kidins220$^{lox/lox\text{-}\Delta Cre}$ astrocytes were treated with 50 ng/ml BDNF for 5 or 30 min or left untreated (time 0). Lysates were analyzed for phosphorylated MAPK1/2 (Thr202/Tyr204; P-MAPK1/2), Akt (Ser473; P-Akt) and PLCγ (Tyr783; P-PLCγ). Membranes were subsequently stripped and re-probed for the total amount of the same protein. The left panel shows representative immunoblots. The middle panel shows the quantification of basal levels of P-MAPK1/2, P-PLCγ and P-Akt in untreated lysates. Data were analyzed as in A and B. The right panel shows the fold-change of phosphorylation for P-MAPK1/2, P-PLCγ and P-Akt upon BDNF stimulation in Kidins220$^{lox/lox\text{-}Cre}$ and Kidins220$^{lox/lox\text{-}\Delta Cre}$ astrocytes compared to levels of phosphorylation in untreated samples for each genotype, set to 1 (dashed line in all graphs). The fold-change of phosphorylation was calculated as described in Fig. 1. For MAPK, we report the sum of MAPK1 and MAPK2 immunoreactivity. *P*>0.05, unpaired Student's *t*-test, *n*=8 independent Kidins220$^{lox/lox}$ cultures. Values are expressed as the means±s.e.m. in all panels.

observed $[Ca^{2+}]_i$ influx was reduced independently of the presence of Kidins220 (Fig. 4F and G; genotype effect: $^{\#}P$=0.0432; K-252a treatment effect: ****P*<0.0001; treatment×genotype interaction: *P*=0.2197, see legend for more details), suggesting that the BDNF-induced $[Ca^{2+}]_i$ variations involved full-length TrkB receptors. BDNF-stimulation in the presence of ANA-12 did not induce any response, confirming that the residual signal was attributable to TrkB-T1 activation (Fig. 4H). Furthermore, the observed response was completely dependent on PLCγ activity, as we did not observe BDNF-induced $[Ca^{2+}]_i$ transients in the presence of the specific PLCγ inhibitor U73122 (Fig. 4I).

Altogether, these data show that BDNF induced modest $[Ca^{2+}]_i$ events in embryonic astrocytes, whereas larger $[Ca^{2+}]_i$ responses are elicited in postnatal cells. Postnatal $[Ca^{2+}]_i$ transients are fully dependent on TrkB receptors, as shown by complete inhibition of TrkB and TrkB-T1 in the presence of ANA-12 (Fig. 4H). Interestingly, part of this response is mediated by the full-length receptor, as shown by the partial reduction of amplitude in the presence of K-252a (Fig. 4F, K-252a treatment effect). Moreover, our results show that Kidins220 plays an active role in this process, as in its absence the amplitude of $[Ca^{2+}]_i$ events is reduced (Fig. 4F, genotype effect).

BDNF stimuli promote gene transcription in postnatal astrocyte cells

To shed light on the functional effects of BDNF signaling in astroglia, we analyzed the transcriptional profile of cultures treated with 1 ng/ml BDNF for three days. We focused on four genes whose expression is crucial for astrocytes physiology, i.e. the excitatory amino acid transporter 2 (*Slc1a2*, hereafter referred to as GLT-1), the ATP-sensitive inward rectifier potassium channel 10 (*Kcnj10*, hereafter referred to as Kir4.1), aquaporin 4 (*Aqp4*) and gap junction alpha-1 protein (*Gja1*, hereafter referred to as Cnx43) (Fig. 5A). Whereas the expression of the genes encoding GLT-1, Kir4 or Cnx43 was insensitive to BDNF, at least within the time frame of our experiment, transcription of *Aqp4* was selectively reduced upon prolonged

Journal of Cell Science (2021) 134, jcs258419. doi:10.1242/jcs.258419

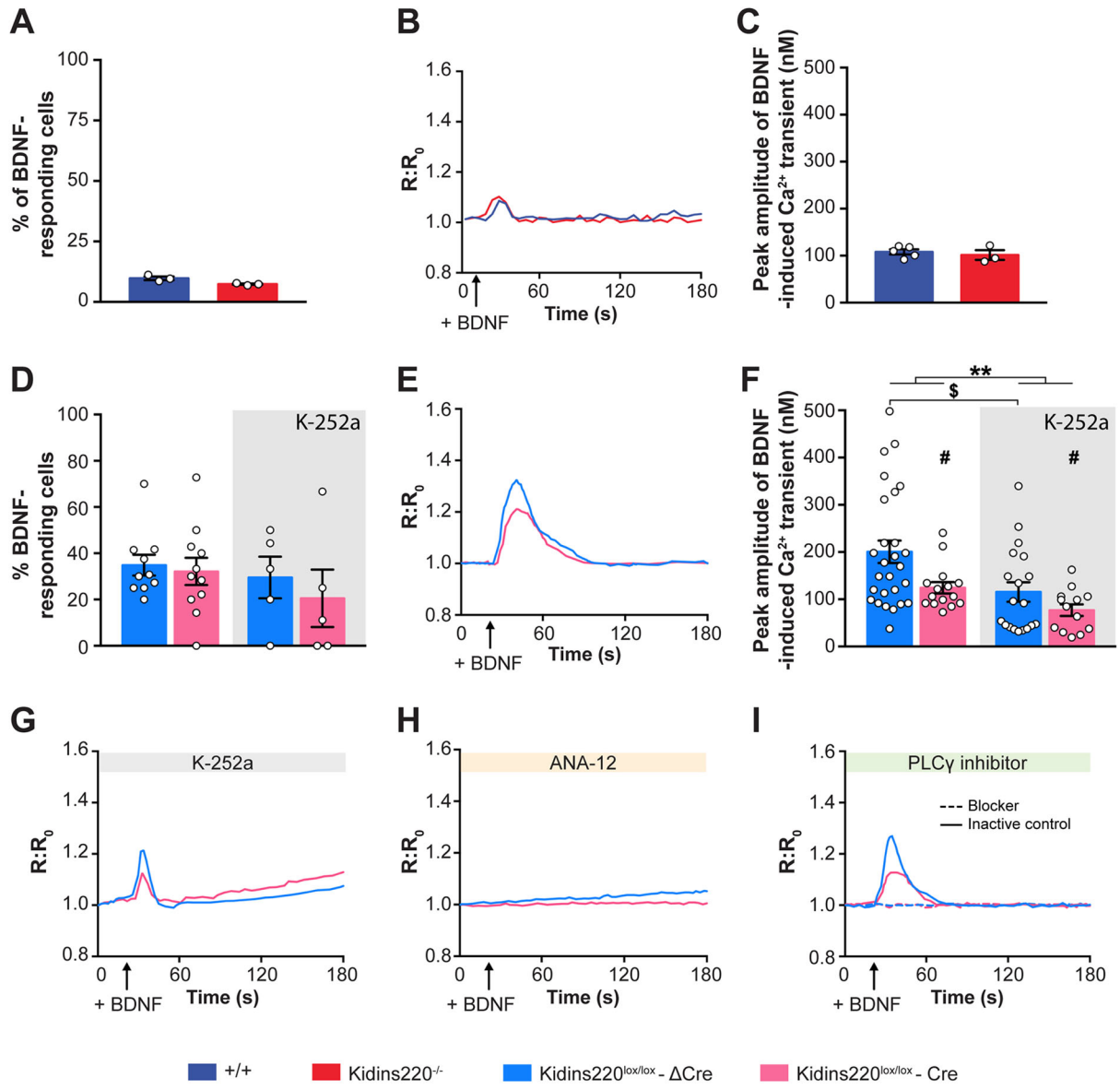

Fig. 4. Depletion of Kidins220 in postnatal cultures impairs BDNF-induced Ca^{2+} transients. (A–C) BDNF-induced $[Ca^{2+}]_i$ transients in embryonic wild-type (+/+) and Kidins220$^{-/-}$ astrocytes. Percentage of cells displaying Ca^{2+} transients in response to BDNF (20 ng/ml) stimulation. *n*=3 for both wild-type and Kidins220$^{-/-}$ cultures (A). $[Ca^{2+}]_i$ transients were defined when R:R_0≥0.025. Time-course of $[Ca^{2+}]_i$ transients (B) and peak amplitude (C) of BDNF-evoked Ca^{2+} levels in wild-type and Kidins220$^{-/-}$ astrocytes. (D–I) BDNF-induced $[Ca^{2+}]_i$ transients in postnatal Kidins220$^{lox/lox\text{-}Cre}$ and Kidins220$^{lox/lox\text{-}\Delta Cre}$ astrocytes. Percentage of cells displaying $[Ca^{2+}]_i$ transients in response to BDNF (20 ng/ml) stimulation in the presence or absence of the tyrosine kinase blocker K-252a (D). *n*=5 and 10 Kidins220$^{lox/lox}$ cultures with and without K-252a, respectively. Time-course of Ca^{2+} transients (E) and peak amplitude (F) of BDNF-evoked Ca^{2+} influx in Kidins220$^{lox/lox\text{-}Cre}$ and Kidins220$^{lox/lox\text{-}\Delta Cre}$ astrocytes in the absence or presence of K-252a. Two-way ANOVA followed by Tukey's multiple comparison test; ***P<0.001 versus untreated, $^{\#}P$<0.05 versus Kidins220$^{lox/lox\text{-}\Delta Cre}$, $^{\$\$\$}P$<0.001 versus untreated Kidins220$^{lox/lox\text{-}\Delta Cre}$ [genotype effect: $F_{(1,62)}$=4.262, $^{\#}P$=0.0432; K-252a treatment effect: $F_{(1,\ 62)}$=20.17, ***P<0.0001; treatment×genotype interaction: $F_{(1,\ 62)}$=1.538, P=0.2197], *n*=27 and 15 cells from six independent cultures for Kidins220$^{lox/lox\text{-}\Delta Cre}$ and Kidins220$^{lox/lox\text{-}Cre}$ cells in the absence of K-252a, and *n*=13 and 11 from six independent cultures for Kidins220$^{lox/lox\text{-}\Delta Cre}$ and Kidins220$^{lox/lox\text{-}Cre}$ cells in the presence of K-252a. Time-course of $[Ca^{2+}]_i$ transients evoked by BDNF in Kidins220$^{lox/lox\text{-}\Delta Cre}$ and Kidins220$^{lox/lox\text{-}Cre}$ astrocytes in the presence of the TrkB receptor kinase inhibitor K-252a (G), the pan-TrkB antagonist ANA-12 (H), the active PLCγ inhibitor U73122 (dashed lines) or its inactive analogue U73343 (solid lines) (I). Values are expressed as the means±s.e.m. in all panels.

stimulation (72 h) with BDNF (*P=0.0153, treatment effect). Although Kidins220 deficiency did not alter the transcription response to BDNF, it selectively and markedly reduced the protein levels of Kir4.1 independently of BDNF ($^{\#\#}P$=0.0067, genotype effect), which was confirmed by western blot analysis (Fig. 5B).

These data suggest that (i) prolonged exposure to BDNF alters the expression of specific astrocyte genes, and that (ii) Kidins220 plays a role in the maintenance of astrocyte homeostasis and K^+ buffering function by modulating the expression of Kir4.1.

Glycolytic metabolism increases in astrocytes during development and is modulated by Kidins220 at the embryonic stage

One of the main functions of astrocytes is to provide neurons with metabolic support, both under physiological conditions and in situations of high energetic demand. Amongst the numerous astrocyte-derived molecules involved in this process, lactate plays a prominent role both as a metabolic and as a signaling molecule (Magistretti and Allaman, 2015). To assess the levels of glycolytic

Journal of Cell Science (2021) 134, jcs258419. doi:10.1242/jcs.258419

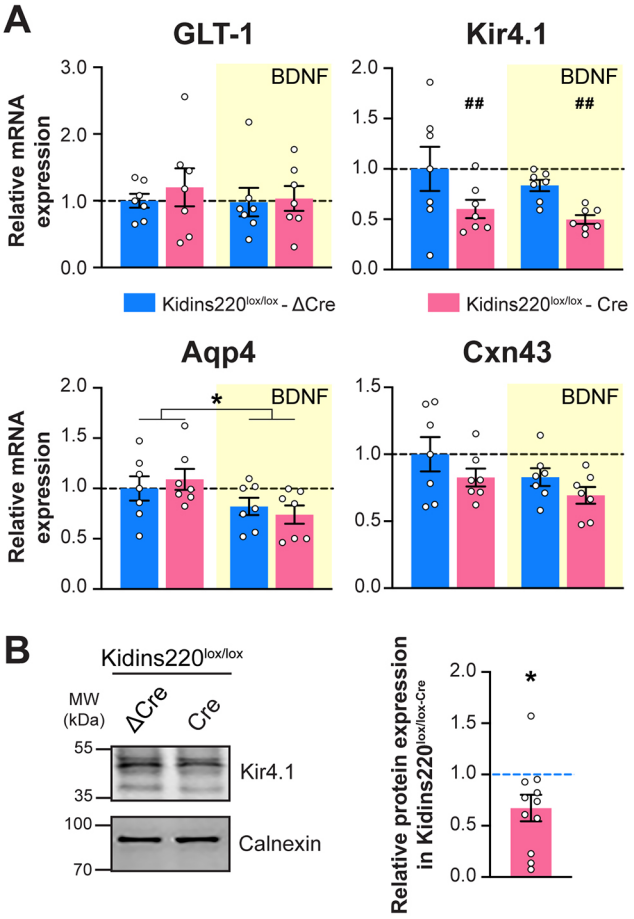

Fig. 5. Transcription of genes encoding Aqp4 or Kir4.1 is reduced in response to prolonged treatment with BDNF or Kidins220 deficiency, respectively, in postnatal astrocytes. (A) mRNA expression profile of *Slc1a2* (GLT-1), *Kcnj10* (Kir4.1), *Aqp4* and *Gja1* (Cnx43) in postnatal Kidins220$^{lox/lox-\Delta Cre}$ and Kidins220$^{lox/lox-Cre}$ astrocytes treated or not with BDNF (1 ng/ml) for 72 h (see Materials and Methods). mRNA levels in the various samples were normalized to respective levels in untreated Kidins220$^{lox/lox-\Delta Cre}$ samples within the same RT-qPCR plate. Two-way ANOVA followed by Tukey's multiple comparison test. **P*<0.05 versus untreated, $^{\#\#}P$<0.01 versus Kidins220$^{lox/lox-\Delta Cre}$. GLT-1: Genotype effect: $F_{(1,\ 24)}$=0.3813, *P*=0.5427; BDNF treatment effect: $F_{(1,\ 24)}$=0.2042, *P*=0.6554; treatment×genotype interaction: $F_{(1,\ 24)}$=0.1262, *P*=0.7255. Kir4.1: Genotype effect: $F_{(1,\ 24)}$=8.817, $^{\#\#}P$=0.0067; BDNF treatment effect: $F_{(1,\ 24)}$=1.179, *P*=0.2883; treatment×genotype interaction: $F_{(1,24)}$=0.06038, *P*=0.8080. Aqp4: Genotype effect: $F_{(1,\ 24)}$=0.002003, *P*=0.9647; BDNF treatment effect: $F_{(1,\ 24)}$=6.817, **P*=0.0153; treatment×genotype interaction: $F_{(1,\ 24)}$=0.7202, *P*=0.4045. Cnx43: Genotype effect: $F_{(1,\ 24)}$=3.302, *P*=0.0817; BDNF treatment effect: $F_{(1,\ 24)}$=3.183, *P*=0.0870; treatment×genotype interaction: $F_{(1,\ 24)}$=0.04637, *P*=0.8313. *n*=7 independent Kidins220$^{lox/lox}$ cultures. (B) Protein extracts from Kidins220$^{lox/lox}$ P0-P1 astrocyte cultures infected with lentiviruses encoding catalytically dead (ΔCre) or active Cre recombinase were analyzed by western blotting using anti-Kir4.1 antibodies and anti-calnexin antibodies as loading control. A representative immunoblot is shown on the left; quantification of immunoreactive bands is on the right. The band intensity from Kidins220$^{lox/lox-Cre}$ samples was normalized to corresponding band intensity from Kidins220$^{lox/lox-\Delta Cre}$ samples within the same nitrocellulose membrane. **P*<0.05, one sample Student's *t*-test, *n*=11 Kidins220$^{lox/lox}$ cultures. Values are expressed as the means±s.e.m. in all panels.

versus oxidative phosphorylation metabolism, we quantified the amount of lactate in the medium of embryonic and postnatal astrocytes, in the presence and absence of Kidins220 (Fig. 6A). Interestingly, we found that, the production of lactate in wild-type postnatal cells is increased compared with that in embryonic cells, suggesting a predominant glycolytic mechanism. Remarkably, Kidins220$^{-/-}$ embryonic cells produce three times more lactate compared to wild-type astrocytes, suggesting impaired mitochondrial metabolism, whereas at the postnatal stage lactate levels in Kidins220-depleted cells are comparable to those in wild-type cultures.

Altogether, these data show that the astrocytic metabolism changes during development by way of increasing the glycolytic power, and reveal a novel and previously unknown role of Kidins220 in cell energy metabolism.

DISCUSSION

The main findings of this work can be summarized as follows. (i) Cultured primary astrocytes predominantly express the TrkB-T1 truncated isoform of the receptor but also express small amounts of full-length signaling-competent TrkB, as shown through BDNF-induced activation of the MAPK pathway; however, expression of TrkB declines in postnatal cells. (ii) Astrocyte cultures show a stage-dependent shift in their response to BDNF, i.e. embryonic cells respond mostly by activation of intracellular signaling pathways (MAPK1/2, PCLγ and Akt) and are unable to induce significant BDNF-dependent $[Ca^{2+}]_i$ transients. Postnatal astrocytes in culture, however, respond to BDNF with the induction of robust $[Ca^{2+}]_i$ transients and the limited activation of intracellular signaling cascades. (iii) The scaffold protein Kidins220 participates in TrkB signaling within both embryonic and postnatal astrocytes, and modulates the transcription of fundamental astrocyte genes, such as that encoding the inward rectifier K^+ channel Kir4.1. A schematic representation of our results is shown in Fig. 6B.

Extensive literature supports the notion that TrkB-T1 is the main isoform expressed in astroglia (Fenner, 2012; Holt et al., 2019); however, experimental evidence also points at a limited expression of the full-length receptor, at least *in vitro* (Climent et al., 2000; Condorelli et al., 1995). Moreover, reactive astrocytes express the full-length TrkB receptor upon CNS injury (McKeon et al., 1997) and in the case of chronic diseases (Soontornniyomkij et al., 1998; Stadelmann et al., 2002), raising the question of whether the astrocyte expression of full-length TrkB under pathological conditions recapitulates intracellular pathways that are normally active during development. Re-activation of developmental programs is, indeed, a known feature of reactive astrocytes (Buffo et al., 2008) and of astrocyte-derived tumors, such as gliomas (Galli et al., 2004; Ignatova et al., 2002; Silver and Steindler, 2009), and the BDNF-TrkB pathway is over-activated in several brain tumors (Meng et al., 2019). Consistent with previous observations (Climent et al., 2000), our data show that the expression of full-length TrkB decreases from embryonic to postnatal astrocytes, supporting the idea that the intracellular pathways activated by this receptor could be active during embryogenesis and are re-activated in the presence of neural pathologies. This finding is potentially relevant in that it shows that cultured astrocytes do retain – to some extent – the identity of the tissue from which they were initially isolated (Schwartz and Nishiyama, 1994; Wu et al., 1998).

Regarding the signaling pathways activated through BDNF in astrocytes, our data indicate activation of the canonical MAPK1/2, PCLγ and Akt pathways is predominant in embryonic cultures. The same cascades are activated to a reduced extent in postnatal cells, which is in agreement with the reduced expression of full-length TrkB. Our embryonic and postnatal cultures are predominantly composed of astrocytes, with only a small (<10%) proportion of other glial cells, mostly microglia (Jaudon et al., 2020). Although

Journal of Cell Science (2021) 134, jcs258419. doi:10.1242/jcs.258419

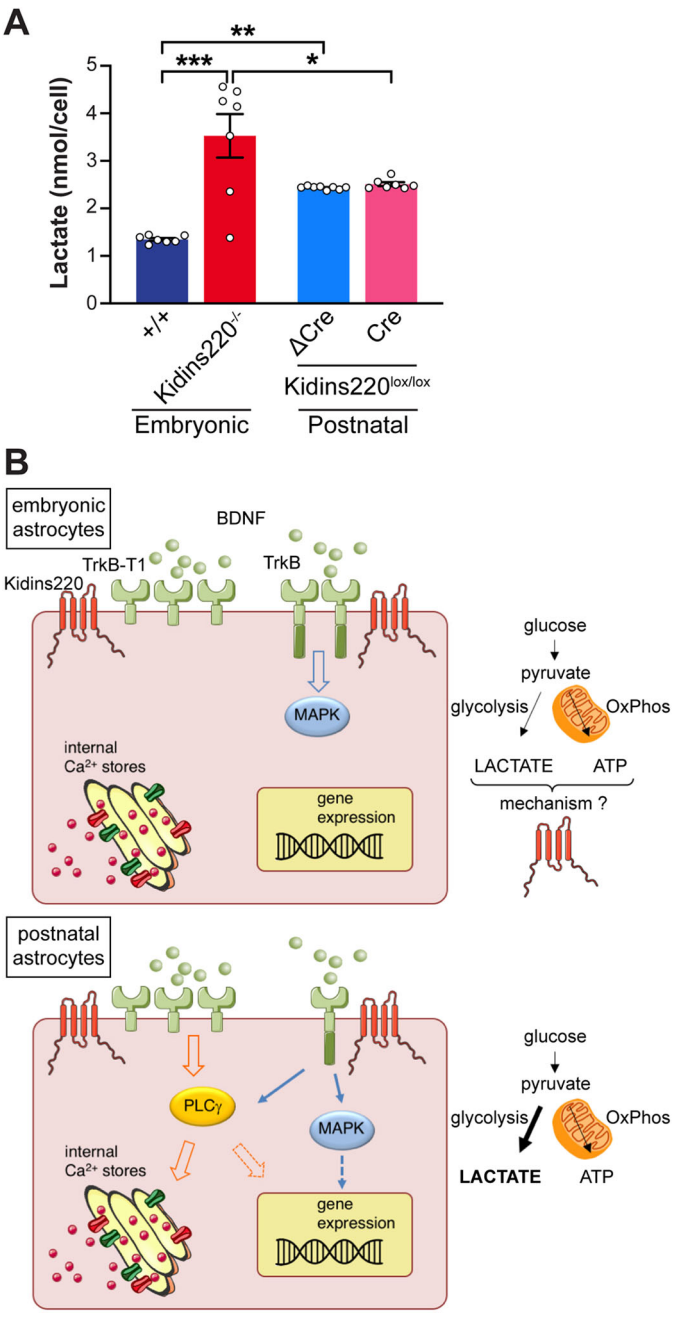

Fig. 6. Kidins220 contributes to cell metabolism and BDNF signaling in astrocytes. (A) Lactate concentration (nmol/cell) was measured in culture medium harvested from confluent cultures of embryonic wild-type (+/+) and Kidins220$^{-/-}$ astrocytes (Embryonic, left), and postnatal Kidins220$^{lox/lox\text{-}\Delta Cre}$ and Kidins220$^{lox/lox\text{-}Cre}$ astrocytes (Postnatal, right). Two-way ANOVA followed by Tukey's multiple comparisons test, *P<0.05, **P<0.01, ***P<0.001. Genotype effect: $F_{(1, 25)}$=25,57, P<0.001; developmental stage effect: $F_{(1, 25)}$=0.02569, P=0.87; genotype×developmental stage interaction: $F_{(1, 25)}$=22,37, P<0.001. n=7-8 cultures. Values are expressed as the means±s.e.m. (B) Schematic, depicting the role of Kidins220 in embryonic (top) and postnatal (bottom) astrocytes. Our model proposes that embryonic astrocytes respond to BDNF stimuli mostly through activation of intracellular signaling cascades via full-length TrkB. In postnatal cells, BDNF mainly activates intracellular $[Ca^{2+}]_i$ transients via TrKB-T1 and PLCγ. Kidins220 contributes to the sustained activation of the MAPK pathway in embryonic cells, whereas it modulates Kidins220 BDNF-induced $[Ca^{2+}]_i$ transients in postnatal cells. Moreover, prolonged treatment with BDNF promotes the transcription of selected genes, such as *Aqp4*, in postnatal cells. During transition from embryonic to postnatal stage, astrocytes increase their glycolytic power and the production of lactate. Kidins220 is involved in controlling the balance between glycolysis and oxidative phosphorylation in embryonic cells, albeit the mechanisms underlying this effect are still unknown.

we cannot exclude a small proportion of activated pathway proteins observed in western blot experiments being derived from cells other than astrocytes, the high levels of phosphorylated pathway proteins and the increased amounts of phosphorylated TrkB in GFAP-positive cells in response to BDNF treatment – revealed by western blotting and fluorescence microscopy, respectively – indicate that the observed changes in intracellular signaling pathways are predominantly attributable to astrocytes. The mechanisms that underlie BDNF-induced $[Ca^{2+}]_i$ transients become fully functional in postnatal astrocytes; indeed, only modest BDNF-induced $[Ca^{2+}]_i$ elevations are observed in embryonic cultures. We hypothesize that such a limited response is ascribable to a still non-functional coupling between Ca^{2+} receptors and channels, on the endoplasmic reticulum and on the plasma membrane, with these together coordinating the mechanism of store-operated Ca^{2+} entry (SOCE) in mature astrocytes (Okubo, 2020). The $[Ca^{2+}]_i$ transients observed upon BDNF administration in postnatal cells comprise two components. The first, which accounts for ∼40% of the observed signal, is mediated by full-length TrkB and sensitive to pre-incubation with K-252a. Complete ablation of $[Ca^{2+}]_i$ transients observed in the presence of the pan-TrkB inhibitor ANA-12 reveals that the second, and predominant, component depends on TrkB-T1, as previously reported (Rose et al., 2003). The complete dependence of $[Ca^{2+}]_i$ variations on PLCγ suggests that pathways activated by both receptors converge upon SOCE. Whereas only 40% of postnatal astrocytes showed responsiveness to BDNF in terms of $[Ca^{2+}]_i$ transients, we found phosphorylated full-length TrkB in the majority of GFAP-positive cells within embryonic cultures. Our Ca^{2+}-imaging data confirmed that the capability of astrocytes to initiate BDNF-induced $[Ca^{2+}]_i$ transients varies, depending on the degree of cell differentiation. Thus, we propose that expression of full-length TrkB is a general feature of embryonic cells. Whether BDNF-responsive astrocytes in postnatal cultures represent a specific subpopulation endowed with distinct physiological functions is a relevant issue that needs to be addressed in future investigations. Interestingly, prolonged treatment with BDNF reduced gene expression of *Aqp4*, indicating that the neurotrophin is capable to induce long-term changes in astrocytes, potentially impacting on their physiology and on their capability to maintain nervous system homeostasis. In contrast to the changes observed regarding the levels of TrkB, levels of p75^{NTR} remained constant in embryonic and postnatal cells. Thus, changes in the amount of p75^{NTR} seem more likely to be linked to injury responses (Cragnolini et al., 2018) than to the developmental stage of the cell.

The scaffold protein Kidins220 is highly expressed in the nervous system during embryonic development and plays a fundamental role in modulating neuronal survival and maturation. Indeed, its complete ablation leads to embryonic lethality with widespread apoptosis in the central and peripheral nervous system (Cesca et al., 2011, 2012). The function of Kidins220 has been extensively studied in neurons, where it contributes to several fundamental processes, such as neuronal differentiation (Higuero et al., 2010), excitability (Cesca et al., 2015) and synaptic plasticity (Scholz-Starke et al., 2012), mostly by mediating BDNF stimuli through its interaction with TrkB and p75^{NTR} (Arevalo et al., 2006, 2004; Kong et al., 2001). In the absence of Kidins220, expression of both TrkB isoforms is reduced in embryonic as well as in postnatal astrocyte

Journal of Cell Science (2021) 134, jcs258419. doi:10.1242/jcs.258419

cultures. In embryonic cultures, Kidins220$^{-/-}$ astrocytes are characterized by reduced sustained activation of the MAPK pathway (Arevalo et al., 2004; Cesca et al., 2012). This suggests that – similar to modulation in neurons – Kidins220 modulates MAPK activation downstream of full-length TrkB in astrocytes. In postnatal astrocytes, Kidins220 affects both TrkB- and TrkB-T1-induced $[Ca^{2+}]_i$ signaling, as both isoforms are reduced in Kidins220-depleted cells. It should be noticed that the interaction between Kidins220 and TrkB involves the transmembrane domain of the receptor (Arevalo et al., 2004), which is shared between the two receptor isoforms. Our gene expression analysis revealed reduced expression of Kir4.1 in Kidins220-depleted astrocytes. In astrocytes, Kir4.1 channels exist as homo-tetramers comprising Kir4.1 subunits as well as hetero-tetramers comprising Kir4.1 and Kir5.1 subunits (Hibino et al., 2004; Patterson et al., 2021). In our quantitative real-time PCR (RT-qPCR) and western blot analysis, we quantified monomeric Kir4.1, which is likely to reflect the abundance of both homo- and hetero-tetramers. Interestingly, similar results have been recently described in cultured astrocytes lacking TrkB-T1 (Aroeira et al., 2015; Holt et al., 2019; Ohira et al., 2007; Vaz et al., 2011). This further supports the notion that Kidins220 and TrkB receptors are part of the same signaling system. Together with the increased expression of transient receptor potential cation channel subfamily V member 4 (TRPV4) previously described by us (Jaudon et al., 2020), this observation suggests that the Kidins220 deficiency subjects astrocytes to a general stress reaction and aids to explain the developmental and activity impairments observed for wild-type neurons when co-cultured with Kidins220$^{-/-}$ cells (Jaudon et al., 2020).

Our data on lactate production raise a number of interesting considerations. For what concerns wild-type cells, our findings are in line with evidence that, in mature astrocytes, production of lactate through anaerobic glycolysis plays a predominant role in astrocyte metabolism (reviewed by Magistretti and Allaman, 2015). For what concerns Kidins220 KO cells, the present findings together with our previous data of reduced ATP secretion in embryonic Kidins220 KO astrocytes (Jaudon et al., 2020), suggest that in KO embryonic astrocytes the balance between glycolysis and oxidative phosphorylation is towards lactate production. This could be indicative of mitochondrial dysfunctions. The mechanisms underlying this effect are presently unknown, and the role of Kidins220 in mitochondria physio-pathology – and, generally, in cellular metabolism – is completely unexplored. The induction and modulation of $[Ca^{2+}]_i$ transients could be a major player, especially given the strict crosstalk between endoplasmic reticulum and mitochondria regarding $[Ca^{2+}]_i$ homeostasis (Verkhratsky et al., 2018).

Overall, our work contributes to understanding the complex and debated mechanisms of neurotrophin signaling in astrocytes, showing that – at least *in vitro* – the full-length and the truncated TrkB receptor are both competent to activate distinct intracellular signaling pathways at distinct stages of astrocyte development. Moreover, we identified Kidins220 as one of the cellular components that endows TrkB and TrkB-T1 signaling specificity. In future studies we will address how these findings translate *in vivo*, under physiological and pathological conditions. In recent years, mutations in the *KIDINS220* gene have been associated with severe neurodevelopmental pathologies, whose main symptoms are intellectual disability and spastic paraplegia (Cesca et al., 2018; El-Dessouky et al., 2020; Jacquemin et al., 2020; Josifova et al., 2016; Mero et al., 2017; Yang et al., 2018; Zhao et al., 2019). Within this context, the observation that Kidins220 controls astrocyte metabolism during embryonic development is instrumental to tackle the pathogenic mechanisms that underlie Kidins220-dependent neurodevelopmental diseases (i.e. SINO syndrome and associated pathologies). A better understanding of the physiological functions of neurotrophins and Kidins220 in neurons and glial cells is instrumental to identify the molecular pathways that lead to this severe neurological disorder.

MATERIALS AND METHODS

Animals

All embryos used in this study were obtained from crosses of Kidins220$^{+/-}$ mice (Cesca et al., 2012; Scholz-Starke et al., 2012) in the C57BL/6 background. Mice were mated overnight and separated in the morning. The development of the embryos was timed from the detection of a vaginal plug, which was considered day 0.5. Postnatal cultures were prepared from P0-P1 pups obtained by crossing Kidins220$^{+/lox}$ mice on the C57BL/6 background. All experiments were carried out according to the guidelines established by the European Community Council (Directive 2010/63/EU of 22 September 2010) and were approved by the Italian Ministry of Health.

Antibodies

The following primary antibodies were used: rabbit polyclonal anti-Kidins220 (1:500; GSC16, #AB34790, Abcam), rabbit polyclonal anti-TrkB (1:1500; #07-225, Millipore), rabbit polyclonal anti-p75^{NTR} (1:2000; #G323A, Promega), rabbit monoclonal anti-phosphorylated TrkB (1:1000; Tyr516, #4619, Cell Signaling), rabbit monoclonal anti-GAPDH (1:10,000; 14C10, #2118, Cell Signaling), rabbit monoclonal anti-phosphorylated MAPK1/2 (1:2000; Thr202/Tyr204, #4377, Cell Signaling), rabbit polyclonal anti-MAPK1/2 (1:2000; #06-182, Millipore), rabbit monoclonal anti-phosphorylated Akt1, Akt2 and Akt3 (1:1000; Ser473, #4058, Cell Signaling), rabbit polyclonal against Akt1, Akt2 and Akt3 (1:1000; #9272, Cell Signaling), rabbit polyclonal anti-phosphorylated PLCγ1 (1:500; Tyr783, #2821, Cell Signaling), rabbit polyclonal anti-PLCγ1 (1:1000; #2822, Cell Signaling), mouse monoclonal anti-glial fibrillary acidic protein (1:500; GFAP, #G3893, Sigma-Aldrich), anti Kir4.1 (1:3000; #APC-035 Alomone Labs) and anti-calnexin (1:5000; #ADI-SPA-860 Enzo Life Sciences).

Secondary antibodies for western blot analysis were ECL Plex goat anti-rabbit IgG-Cy5 (1:2500; PA45012, GE Healthcare), ECL Plex goat anti-mouse IgG-Cy3 (1:2500; PA43009, GE Healthcare), HRP-conjugated goat anti-rabbit antibodies (1:5000; #31460, ThermoFisher Scientific) and HRP-conjugated goat anti-mouse antibodies (1:5000; #31430, Thermo Fisher Scientific). Fluorescent secondary antibodies for immunocytochemistry were from Molecular Probes (Thermo Fisher Scientific; Alexa Fluor 488, 1:500, #A11029; Alexa Fluor 647, 1:500, #A21450). Hoechst 33342 (1 mg/ml; #B2261, Sigma-Aldrich) was used to stain nuclei.

Primary astrocyte culture

E18.5 or P0-P1 cortices were dissected in ice-cold PBS, incubated with trypsin 0.25% and 1 mg/ml DNase I for 30 min at 37°C, and mechanically dissociated. Cells were then re-suspended and plated on poly-D-lysine-coated flasks or glass coverslips, in Minimum Essential Medium (MEM) containing 10% FBS, 2 mM glutamine, 33 mM glucose and antibiotics (astrocyte culture medium). After 24 h, the medium was removed and replaced with fresh culture medium. After 1 week, half of the medium was replaced with fresh culture medium. Embryonic and postnatal cultures comprised ∼90% astrocytes and were totally devoid of neurons (Jaudon et al., 2020).

Lentivirus production and infection procedures

HEK293T (ATCC CRL-3216) cells were maintained in Iscove's Modified Dulbecco's Medium (IMDM) supplemented with 10% FBS, 2 mM glutamine, 100 U/ml penicillin and 0.1 mg/ml streptomycin in a 5% CO_2 humidified incubator at 37°C. Cells were routinely tested and resulted mycoplasma free. Cells were transfected with the Δ8.9 encapsidation plasmid, the VSVG envelope plasmid and the pLenti-PGK-Cre-EGFP or

Journal of Cell Science (2021) 134, jcs258419. doi:10.1242/jcs.258419

pLenti-PGK-ΔCre-EGFP plasmids (Kaeser et al., 2011) using the calcium phosphate method. Transfection medium was replaced with fresh medium after 16 h. Supernatants were collected between 36 and 48 h after transfection, centrifuged to remove cell debris, passed through a 0.45 µm filter and ultracentrifuged 2 h at 20,000 ***g*** at 4°C. Viral pellets were re-suspended in PBS, aliquoted and stored at −80°C until use.

Confluent postnatal cultures were trypsinized and seeded on 6-well plates or glass coverslips coated with poly-D-lysine for subsequent experiments. Cells were infected 3 days later with lentiviruses encoding catalytically dead (ΔCre) or active Cre recombinase with the lowest infectious dose capable of transducing ≥95% of cells (dilution range 1:500 to 1:800) and used for experiments ≥7 days after transduction.

Calcium imaging

Astrocytes at 3 DIV or at 7–8 DIV after lentivirus infection were loaded with 1 µg/ml Fura-2-AM (#F1221, ThermoFisher) in astrocyte culture medium for 30 min at 37°C. Subsequently, cells were washed in recording buffer (10 mM HEPES pH 7.4, 150 mM NaCl, 3 mM KCl, 1 mM $MgCl_2$, 10 mM glucose and 2 mM $CaCl_2$) 30 min at 37°C to allow hydrolysis of the esterified groups. Coverslips with cells were mounted on the imaging chamber and loaded with 0.45 ml of recording buffer. Fura-2-loaded cultures were observed with an inverted Leica 6000 microscope using a HCX PL APO lambda blue 63.0×1.40 oil-immersion objective. For analyzing BDNF-evoked Ca^{2+} transients, 50 µl of BDNF solution [final concentration 20 ng/ml, as reported in Rose et al. (2003), #B3795, Sigma] were manually added to the culture medium 15 s after the beginning of the recordings. Where indicated, cells were pre-incubated with 150 nM K-252a (tyrosine kinase blocker, #K1639, Sigma), 1 µM ANA-12 (TrkB receptor antagonist, #SML0209, Sigma), 10 µM U73122 (PLCγ inhibitor, #U6756, Sigma) or 10 µM U73343 (inactive analog, #U6881, Sigma) for 10 min before the beginning of the recordings. Samples were excited at 340 and 380 nm and images of fluorescence emission at 510 nm were acquired using a Hamamatsu-C9100-02-LNK00 camera. Ca^{2+} levels were estimated from background subtracted ratio images (340/380 nm) of Fura-2-loaded astrocytes at the cell body level according to the equation by Grynkiewicz (Grynkiewicz et al., 1985):

$$[Ca^{2+}] = K_d \times \frac{R - R_{min}}{R_{max} - R} \times \frac{F^{380}_{max}}{F^{380}_{min}}, \quad (1)$$

where R is the measured ratio of 340 to 380 nm; R_{min} and R_{max} are the ratios in the absence of Ca^{2+} or when Fura-2 is saturated by Ca^{2+}, and F^{380}_{max} and F^{380}_{min} are the fluorescence intensities when Ca^{2+} levels =0 or saturated at excitation of 380 nm. To determine the binding affinity K_d in our system, *in situ* calibration was performed by using 1 µM of the Ca^{2+}-ionophore ionomycin in recording buffer containing increasing Ca^{2+} concentrations in the range of 1 nM–10 mM. $[Ca^{2+}]_i$ transients were defined for $R:R_0 \geq 0.025$, with R_0 the basal fluorescence intensity before the stimulus.

Biochemical techniques

Cells were washed once in ice-cold PBS and lysed in RIPA buffer (50 mM Tris-HCl pH 7.4, 150 mM NaCl, 2 mM EDTA, 1% NP40, 0.1% SDS) plus protease and phosphatase inhibitors (complete EDTA-free protease inhibitors, Roche Diagnostic; serine/threonine phosphatase inhibitor and tyrosine phosphatase inhibitor, Sigma). After centrifugation at 16,000 ***g*** for 15 min at 4°C, protein concentration was quantified using the BCA Protein Assay kit (ThermoFisher Scientific). SDS-PAGE and western blotting were performed using precast 4–12% NuPAGE Novex Bis-Tris Gels (Invitrogen). After incubation with primary antibodies, membranes were incubated with fluorescent secondary antibodies and revealed by a Typhoon Variable Mode Imager (GE Healthcare) or with HRP-conjugated secondary antibodies and ECL Prime Western Blotting System (#RPN2106, GE Healthcare) and imaged using a ChemiDoc imaging system (Biorad). Immunoreactive bands were quantified using ImageJ software. The fold-change of activation was calculated by first calculating the intensity ratio of phosphorylated bands to the total amount of corresponding protein for each sample, and then by dividing the ratios of phosphorylated to total treated samples by the ratio of phosphorylated to total untreated control samples.

Immunocytochemistry and image analysis

Cells were fixed in 4% PFA for 15 min, then washed in PBS. Cells were subsequently permeabilized with 0.2% Triton X-100 in PBS for 10 min at room temperature (RT) then incubated with primary antibodies diluted in PBS 1% BSA overnight at 4°C or 2 h at RT. After five washes in PBS, cells were incubated with fluorescent secondary antibodies diluted in PBS 1% BSA. After washes, coverslips were mounted with Mowiol.

Confocal stacks were acquired with a Leica SP8 using a 40× oil immersion objective (NA 1.40), with 1 µm between optical sections. Images were analyzed using ImageJ software. The maximal fluorescence intensities of in-focus stacks were *z*-projected and the resulting images were automatically thresholded. Regions of interests were manually drawn around the borders of GFAP-positive cells in the red channel; fluorescence intensity was measured in the green channel (P-TrkB). Quantification was performed on 18–20 fields per condition from three independent cell preparations. Data are reported as the average P-TrkB fluorescence intensity of all GFAP-positive cells in each field.

Prolonged BDNF treatment, RNA extraction and RT-qPCR

Three days after lentiviral infection, $Kidins220^{lox/lox}$ astrocytes cultures were serum starved overnight then treated with 1 ng/ml BDNF on the following morning or left untreated. Treatment was repeated on the next 2 days and total RNA was extracted on the third day with the QIAzol lysis reagent (Qiagen). The corresponding cDNAs were prepared by reverse transcription of 1 µg of RNA using the SuperScript III First-Strand Synthesis System (Invitrogen) with an oligo-dT primer according to the manufacturer's instructions. The resulting cDNAs were used as a template for RT-qPCR using a CFX96 Real-Time PCR Detection System (Biorad) with a SYBR Green master mix (Qiagen). Thermal cycling parameters were 5 min at 95°C, followed by 40 cycles of 95°C for 15 s, and 60°C for 45 s. The relative quantification in gene expression was determined using the ΔΔCt method. Data were normalized to Transferrin receptor protein 1 (TRFR), TATA-box-binding protein (TBP), and Tubulin beta-2A (TUBB2) by the multiple internal control gene method with GeNorm algorithm (Vandesompele et al., 2002). Sequences of the primers used are listed in Table S1.

Lactate assay

Lactate contents were measured using an L-Lactate assay kit (#MAK064, Sigma) according to the manufacturer's instructions. Culture medium was collected from confluent cultures, filtered through a 30 kDa cut-off spin filter and stored at −80°C until processing. Reaction reagents were prepared as instructed and mixed with 50 µL of the samples, incubated at room temperature for 30 min protected from light, and measured at OD 570 nm. Lactate concentration was normalized to the number of cells.

Statistical analysis

Data are presented as the means±standard error of the means (±s.e.m.) throughout the text. Data distribution was assessed using the D'Agostino-Pearson omnibus normality test. When comparing two groups, unpaired two-sided Student's *t*-test and one-sample *t*-test were used; equality of variances was assessed by using the F test. When more than two groups were compared, two-way ANOVA followed by Tukey's post-hoc multiple comparison test was performed to assess significance as indicated in figure legends; equality of variances was assessed by using the Brown-Forsythe's and Bartlett's test. Alpha levels for all tests were 0.05% (95% confidence intervals). No statistical methods were used to predetermine sample sizes; however, sample sizes used for the experiments described here (indicated in figure legends) were similar to those previously reported in the literature for similar experiments. The ROUT method with Q=1% was used to identify outliers for exclusion from analysis. All statistical procedures were performed using GraphPad Prism 7 software (GraphPad Software, Inc).

Acknowledgements

We kindly acknowledge Drs A. Mehilli, D. Moruzzo and R. Navone for help with maintenance, breeding and genotyping of the Kidins220 mouse strains; and Drs R. Ciancio and I. Dallorto for the administrative support.

Competing interests
The authors declare no competing or financial interests.

Author contributions
Conceptualization: F.J., S.F., F.B., F.C.; Methodology: F.J., M.A.; Validation: F.J., M.A.; Formal analysis: F.J., M.A.; Investigation: F.J., M.A.; Data curation: F.J., M.A.; Writing - original draft: F.J., S.F., F.C.; Writing - review & editing: F.B., F.C.; Visualization: F.J.; Supervision: F.C.; Project administration: F.C.; Funding acquisition: F.B., F.C.

Funding
The study was supported by research grants from: IRCCS Ospedale Policlinico San Martino (Ricerca Corrente and '5×1000' to F.C. and F.B.), the Ministero dell'Istruzione, dell'Università e della Ricerca (grant no. PRIN 2017-A9MK4R to F.B.), Compagnia di San Paolo (grant no. 2013.1014 to F.C.).

Data availability
The datasets used and/or analyzed during the current study are available from the corresponding author on reasonable request.

Peer review history
The peer review history is available online at https://journals.biologists.com/jcs/article-lookup/doi/10.1242/jcs.258419

References

Arévalo, J. C., Yano, H., Teng, K. K. and Chao, M. V. (2004). A unique pathway for sustained neurotrophin signaling through an ankyrin-rich membrane-spanning protein. *EMBO J.* **23**, 2358-2368. doi:10.1038/sj.emboj.7600253

Arévalo, J. C., Pereira, D. B., Yano, H., Teng, K. K. and Chao, M. V. (2006). Identification of a switch in neurotrophin signaling by selective tyrosine phosphorylation. *J. Biol. Chem.* **281**, 1001-1007. doi:10.1074/jbc.M504163200

Aroeira, R. I., Sebastião, A. M. and Valente, C. A. (2015). BDNF, via truncated TrkB receptor, modulates GlyT1 and GlyT2 in astrocytes. *Glia* **63**, 2181-2197. doi:10.1002/glia.22884

Bergami, M., Santi, S., Formaggio, E., Cagnoli, C., Verderio, C., Blum, R., Berninger, B., Matteoli, M. and Canossa, M. (2008). Uptake and recycling of pro-BDNF for transmitter-induced secretion by cortical astrocytes. *J. Cell Biol.* **183**, 213-221. doi:10.1083/jcb.200806137

Buffo, A., Rite, I., Tripathi, P., Lepier, A., Colak, D., Horn, A.-P., Mori, T. and Götz, M. (2008). Origin and progeny of reactive gliosis: a source of multipotent cells in the injured brain. *Proc. Natl. Acad. Sci. USA* **105**, 3581-3586. doi:10.1073/pnas.0709002105

Cazorla, M., Prémont, J., Mann, A., Girard, N., Kellendonk, C. and Rognan, D. (2011). Identification of a low-molecular weight TrkB antagonist with anxiolytic and antidepressant activity in mice. *J. Clin. Invest.* **121**, 1846-1857. doi:10.1172/JCI43992

Cesca, F., Yabe, A., Spencer-Dene, B., Arrigoni, A., Al-Qatari, M., Henderson, D., Phillips, H., Koltzenburg, M., Benfenati, F. and Schiavo, G. (2011). Kidins220/ARMS is an essential modulator of cardiovascular and nervous system development. *Cell Death Dis.* **2**, e226. doi:10.1038/cddis.2011.108

Cesca, F., Yabe, A., Spencer-Dene, B., Scholz-Starke, J., Medrihan, L., Maden, C. H., Gerhardt, H., Orriss, I. R., Baldelli, P., Al-Qatari, M. et al. (2012). Kidins220/ARMS mediates the integration of the neurotrophin and VEGF pathways in the vascular and nervous systems. *Cell Death Differ.* **19**, 194-208. doi:10.1038/cdd.2011.141

Cesca, F., Satapathy, A., Ferrea, E., Nieus, T., Benfenati, F. and Scholz-Starke, J. (2015). Functional interaction between the scaffold protein Kidins220/ARMS and neuronal voltage-gated Na+ channels. *J. Biol. Chem.* **290**, 18045-18055. doi:10.1074/jbc.M115.654699

Cesca, F., Schiavo, G. and Benfenati, F. (2018). Kidins220/ARMS transgenic lines could be instrumental in the understanding of the molecular mechanisms leading to spastic paraplegia and obesity. *Eur. J. Neurol.* **25**, e107. doi:10.1111/ene.13693

Climent, E., Sancho-Tello, M., Miñana, R., Barettino, D. and Guerri, C. (2000). Astrocytes in culture express the full-length Trk-B receptor and respond to brain derived neurotrophic factor by changing intracellular calcium levels: effect of ethanol exposure in rats. *Neurosci. Lett.* **288**, 53-56. doi:10.1016/S0304-3940(00)01207-6

Colombo, E. and Farina, C. (2016). Astrocytes: key regulators of neuroinflammation. *Trends Immunol.* **37**, 608-620. doi:10.1016/j.it.2016.06.006

Colombo, E., Cordiglieri, C., Melli, G., Newcombe, J., Krumbholz, M., Parada, L. F., Medico, E., Hohlfeld, R., Meinl, E. and Farina, C. (2012). Stimulation of the neurotrophin receptor TrkB on astrocytes drives nitric oxide production and neurodegeneration. *J. Exp. Med.* **209**, 521-535. doi:10.1084/jem.20110698

Condorelli, D. F., Dell'Albani, P., Mudò, G., Timmusk, T. and Belluardo, N. (1994). Expression of neurotrophins and their receptors in primary astroglial cultures: induction by cyclic AMP-elevating agents. *J. Neurochem.* **63**, 509-516. doi:10.1046/j.1471-4159.1994.63020509.x

Condorelli, D. F., Salin, T., Dell'Albani, P., Mudò, G., Corsaro, M., Timmusk, T., Metsis, M. and Belluardo, N. (1995). Neurotrophins and their trk receptors in cultured cells of the glial lineage and in white matter of the central nervous system. *J. Mol. Neurosci.* **6**, 237-248. doi:10.1007/BF02736783

Cragnolini, A. B. and Friedman, W. J. (2008). The function of p75NTR in glia. *Trends Neurosci.* **31**, 99-104. doi:10.1016/j.tins.2007.11.005

Cragnolini, A. B., Montenegro, G., Friedman, W. J. and Mascó, D. H. (2018). Brain-region specific responses of astrocytes to an in vitro injury and neurotrophins. *Mol. Cell. Neurosci.* **88**, 240-248. doi:10.1016/j.mcn.2018.02.007

Dallérac, G., Zapata, J. and Rouach, N. (2018). Versatile control of synaptic circuits by astrocytes: where, when and how? *Nat. Rev. Neurosci.* **19**, 729-743. doi:10.1038/s41583-018-0080-6

El-Dessouky, S. H., Issa, M. Y., Aboulghar, M. M., Gaafar, H. M., Elarab, A. E., Ateya, M. I., Omar, H. H., Beetz, C. and Zaki, M. S. (2020). Prenatal delineation of a distinct lethal fetal syndrome caused by a homozygous truncating *KIDINS220* variant. *Am. J. Med. Genet. A* **182**, 2867-2876. doi:10.1002/ajmg.a.61858

Fenner, B. M. (2012). Truncated TrkB: beyond a dominant negative receptor. *Cytokine Growth Factor. Rev.* **23**, 15-24. doi:10.1016/j.cytogfr.2012.01.002

Galli, R., Binda, E., Orfanelli, U., Cipelletti, B., Gritti, A., De Vitis, S., Fiocco, R., Foroni, C., Dimeco, F. and Vescovi, A. (2004). Isolation and characterization of tumorigenic, stem-like neural precursors from human glioblastoma. *Cancer Res.* **64**, 7011-7021. doi:10.1158/0008-5472.CAN-04-1364

Grynkiewicz, G., Poenie, M. and Tsien, R. Y. (1985). A new generation of Ca2+ indicators with greatly improved fluorescence properties. *J. Biol. Chem.* **260**, 3440-3450. doi:10.1016/S0021-9258(19)83641-4

Hibino, H., Fujita, A., Iwai, K., Yamada, M. and Kurachi, Y. (2004). Differential assembly of inwardly rectifying K+ channel subunits, Kir4.1 and Kir5.1, in brain astrocytes. *J. Biol. Chem.* **279**, 44065-44073. doi:10.1074/jbc.M405985200

Higuero, A. M., Sanchez-Ruiloba, L., Doglio, L. E., Portillo, F., Abad-Rodríguez, J., Dotti, C. G. and Iglesias, T. (2010). Kidins220/ARMS modulates the activity of microtubule-regulating proteins and controls neuronal polarity and development. *J. Biol. Chem.* **285**, 1343-1357. doi:10.1074/jbc.M109.024703

Holt, L. M., Hernandez, R. D., Pacheco, N. L., Torres Ceja, B., Hossain, M. and Olsen, M. L. (2019). Astrocyte morphogenesis is dependent on BDNF signaling via astrocytic TrkB.T1. *eLife* **8**, e44667. doi:10.7554/eLife.44667

Hutton, L. A., deVellis, J. and Perez-Polo, J. R. (1992). Expression of p75NGFR TrkA, and TrkB mRNA in rat C6 glioma and type I astrocyte cultures. *J. Neurosci Res.* **32**, 375-383. doi:10.1002/jnr.490320309

Ignatova, T. N., Kukekov, V. G., Laywell, E. D., Suslov, O. N., Vrionis, F. D. and Steindler, D. A. (2002). Human cortical glial tumors contain neural stem-like cells expressing astroglial and neuronal markers in vitro. *Glia* **39**, 193-206. doi:10.1002/glia.10094

Inoue, S., Susukida, M., Ikeda, K., Murase, K. and Hayashi, K. (1997). Dopaminergic transmitter up-regulation of brain-derived neurotrophic factor (BDNF) and nerve growth factor (NGF) synthesis in mouse astrocytes in culture. *Biochem. Biophys. Res. Commun.* **238**, 468-472. doi:10.1006/bbrc.1997.7324

Jacquemin, V., Antoine, M., Duerinckx, S., Massart, A., Desir, J., Perazzolo, C., Cassart, M., Thomas, D., Segers, V., Lecomte, S. et al. (2020). TrkA mediates effect of novel KIDINS220 mutation in human brain ventriculomegaly. *Hum. Mol. Genet.* **29**, 3757-3764. doi:10.1093/hmg/ddaa245

Jaudon, F., Chiacchiaretta, M., Albini, M., Ferroni, S., Benfenati, F. and Cesca, F. (2020). Kidins220/ARMS controls astrocyte calcium signaling and neuron–astrocyte communication. *Cell Death Differ.* **27**, 1505-1519. doi:10.1038/s41418-019-0431-5

Jean, Y. Y., Lercher, L. D. and Dreyfus, C. F. (2008). Glutamate elicits release of BDNF from basal forebrain astrocytes in a process dependent on metabotropic receptors and the PLC pathway. *Neuron Glia Biol.* **4**, 35-42. doi:10.1017/S1740925X09000052

Josifova, D. J., Monroe, G. R., Tessadori, F., de Graaff, E., van der Zwaag, B., Mehta, S. G., The DDD Study, Harakalova, M., Duran, K. J., Savelberg, S. M. C. et al. (2016). Heterozygous KIDINS220/ARMS nonsense variants cause spastic paraplegia, intellectual disability, nystagmus, and obesity. *Hum. Mol. Genet.* **25**, 2158-2167. doi:10.1093/hmg/ddw082

Kaeser, P. S., Deng, L., Wang, Y., Dulubova, I., Liu, X., Rizo, J. and Südhof, T. C. (2011). RIM proteins tether Ca2+ channels to presynaptic active zones via a direct PDZ-domain interaction. *Cell* **144**, 282-295. doi:10.1016/j.cell.2010.12.029

Kinboshi, M., Mukai, T., Nagao, Y., Matsuba, Y., Tsuji, Y., Tanaka, S., Tokudome, K., Shimizu, S., Ito, H., Ikeda, A. et al. (2017). Inhibition of inwardly rectifying potassium (Kir) 4.1 channels facilitates Brain-Derived Neurotrophic Factor (BDNF) expression in astrocytes. *Front. Mol. Neurosci.* **10**, 408. doi:10.3389/fnmol.2017.00408

Kong, H., Boulter, J., Weber, J. L., Lai, C. and Chao, M. V. (2001). An evolutionarily conserved transmembrane protein that is a novel downstream target of neurotrophin and ephrin receptors. *J. Neurosci.* **21**, 176-185. doi:10.1523/JNEUROSCI.21-01-00176.2001

Magistretti, P. J. and Allaman, I. (2015). A cellular perspective on brain energy metabolism and functional imaging. *Neuron* **86**, 883-901. doi:10.1016/j.neuron.2015.03.035

Matyas, J. J., O'Driscoll, C. M., Yu, L., Coll-Miro, M., Daugherty, S., Renn, C. L., Faden, A. I., Dorsey, S. G. and Wu, J. (2017). Truncated TrkB.T1-Mediated astrocyte dysfunction contributes to impaired motor function and neuropathic pain after spinal cord injury. *J. Neurosci.* **37**, 3956-3971. doi:10.1523/JNEUROSCI.3353-16.2017

McKeon, R. J., Silver, J. and Large, T. H. (1997). Expression of full-length trkB receptors by reactive astrocytes after chronic CNS injury. *Exp. Neurol.* **148**, 558-567. doi:10.1006/exnr.1997.6698

Meng, L., Liu, B., Ji, R., Jiang, X., Yan, X. and Xin, Y. (2019). Targeting the BDNF/TrkB pathway for the treatment of tumors. *Oncol. Lett.* **17**, 2031-2039. doi:10.3892/ol.2018.9854

Mero, I.-L., Mørk, H. H., Sheng, Y., Blomhoff, A., Opheim, G. L., Erichsen, A., Vigeland, M. D. and Selmer, K. K. (2017). Homozygous KIDINS220 loss-of-function variants in fetuses with cerebral ventriculomegaly and limb contractures. *Hum. Mol. Genet.* **26**, 3792-3796. doi:10.1093/hmg/ddx263

Miklič, S., Jurič, D. M. and Čarman-Kržan, M. (2004). Differences in the regulation of BDNF and NGF synthesis in cultured neonatal rat astrocytes. *Int. J. Dev. Neurosci.* **22**, 119-130. doi:10.1016/j.ijdevneu.2004.03.001

Neubrand, V. E., Cesca, F., Benfenati, F. and Schiavo, G. (2012). Kidins220/ARMS as a functional mediator of multiple receptor signalling pathways. *J. Cell Sci.* **125**, 1845-1854. doi:10.1242/jcs.102764

Ohira, K., Kumanogoh, H., Sahara, Y., Homma, K. J., Hirai, H., Nakamura, S. and Hayashi, M. (2005). A truncated tropo-myosin-related kinase B receptor, T1, regulates glial cell morphology via Rho GDP dissociation inhibitor 1. *J. Neurosci.* **25**, 1343-1353. doi:10.1523/JNEUROSCI.4436-04.2005

Ohira, K., Funatsu, N., Homma, K. J., Sahara, Y., Hayashi, M., Kaneko, T. and Nakamura, S. (2007). Truncated TrkB-T1 regulates the morphology of neocortical layer I astrocytes in adult rat brain slices. *Eur. J. Neurosci.* **25**, 406-416. doi:10.1111/j.1460-9568.2007.05282.x

Okubo, Y. (2020). Astrocytic Ca^{2+} signaling mediated by the endoplasmic reticulum in health and disease. *J. Pharmacol. Sci.* **144**, 83-88. doi:10.1016/j.jphs.2020.07.006

Park, H. and Poo, M.-M. (2013). Neurotrophin regulation of neural circuit development and function. *Nat. Rev. Neurosci.* **14**, 7-23. doi:10.1038/nrn3379

Patterson, K. C., Kahanovitch, U., Gonçalves, C. M., Hablitz, J. J., Staruschenko, A., Mulkey, D. K. and Olsen, M. L. (2021). Kir 5.1-dependent CO_2/H^+ -sensitive currents contribute to astrocyte heterogeneity across brain regions. *Glia* **69**, 310-325. doi:10.1002/glia.23898

Pöyhönen, S., Er, S., Domanskyi, A. and Airavaara, M. (2019). Effects of neurotrophic factors in glial cells in the central nervous system: expression and properties in neurodegeneration and injury. *Front. Physiol.* **10**, 486. doi:10.3389/fphys.2019.00486

Rose, C. R., Blum, R., Pichler, B., Lepier, A., Kafitz, K. W. and Konnerth, A. (2003). Truncated TrkB-T1 mediates neurotrophin-evoked calcium signalling in glia cells. *Nature* **426**, 74-78. doi:10.1038/nature01983

Rousseaud, A., Delépine, C., Nectoux, J., Billuart, P. and Bienvenu, T. (2015). Differential expression and regulation of Brain-Derived Neurotrophic Factor (*BDNF*) mRNA isoforms in brain cells from $Mecp2^{308/y}$ mouse model. *J. Mol. Neurosci.* **56**, 758-767. doi:10.1007/s12031-014-0487-0

Saba, J., López Couselo, F., Turati, J., Carniglia, L., Durand, D., de Laurentiis, A., Lasaga, M. and Caruso, C. (2020). Astrocytes from cortex and striatum show differential responses to mitochondrial toxin and BDNF: implications for protection of striatal neurons expressing mutant huntingtin. *J. Neuroinflammation* **17**, 290. doi:10.1186/s12974-020-01965-4

Saha, R. N., Liu, X. and Pahan, K. (2006). Up-regulation of BDNF in astrocytes by TNF-α: a case for the neuroprotective role of cytokine. *J. Neuroimmune Pharmacol.* **1**, 212-222. doi:10.1007/s11481-006-9020-8

Santello, M., Toni, N. and Volterra, A. (2019). Astrocyte function from information processing to cognition and cognitive impairment. *Nat. Neurosci.* **22**, 154-166. doi:10.1038/s41593-018-0325-8

Scholz-Starke, J. and Cesca, F. (2016). Stepping out of the shade: control of neuronal activity by the scaffold protein Kidins220/ARMS. *Front. Cell Neurosci.* **10**, 68. doi:10.3389/fncel.2016.00068

Scholz-Starke, J., Cesca, F., Schiavo, G., Benfenati, F. and Baldelli, P. (2012). Kidins220/ARMS is a novel modulator of short-term synaptic plasticity in hippocampal GABAergic neurons. *PLoS ONE* **7**, e35785. doi:10.1371/journal.pone.0035785

Schwartz, J. P. and Nishiyama, N. (1994). Neurotrophic factor gene expression in astrocytes during development and following injury. *Brain Res. Bull.* **35**, 403-407. doi:10.1016/0361-9230(94)90151-1

Silver, D. J. and Steindler, D. A. (2009). Common astrocytic programs during brain development, injury and cancer. *Trends Neurosci.* **32**, 303-311. doi:10.1016/j.tins.2009.01.008

Soontornniyomkij, V., Wang, G., Pittman, C. A., Wiley, C. A. and Achim, C. L. (1998). Expression of brain-derived neurotrophic factor protein in activated microglia of human immunodeficiency virus type 1 encephalitis. *Neuropathol. Appl. Neurobiol.* **24**, 453-460. doi:10.1046/j.1365-2990.1998.00134.x

Stadelmann, C., Kerschensteiner, M., Misgeld, T., Brück, W., Hohlfeld, R. and Lassmann, H. (2002). BDNF and gp145trkB in multiple sclerosis brain lesions: neuroprotective interactions between immune and neuronal cells? *Brain* **125**, 75-85. doi:10.1093/brain/awf015

Vandesompele, J., De Preter, K., Pattyn, F., Poppe, B., Van Roy, N., De Paepe, A. and Speleman, F. (2002). Accurate normalization of real-time quantitative RT-PCR data by geometric averaging of multiple internal control genes. *Genome Biol.* **3**, research0034. doi:10.1186/gb-2002-3-7-research0034

Vaz, S. H., Jørgensen, T. N., Cristóvão-Ferreira, S., Duflot, S., Ribeiro, J. A., Gether, U. and Sebastiaã, A. M. (2011). Brain-derived neurotrophic factor (BDNF) enhances GABA transport by modulating the trafficking of GABA transporter-1 (GAT-1) from the plasma membrane of rat cortical astrocytes. *J. Biol. Chem.* **286**, 40464-40476. doi:10.1074/jbc.M111.232009

Verkhratsky, A., Matteoli, M., Parpura, V., Mothet, J. P. and Zorec, R. (2016). Astrocytes as secretory cells of the central nervous system: idiosyncrasies of vesicular secretion. *EMBO J.* **35**, 239-257. doi:10.15252/embj.201592705

Verkhratsky, A., Trebak, M., Perocchi, F., Khananshvili, D. and Sekler, I. (2018). Crosslink between calcium and sodium signalling. *Exp. Physiol.* **103**, 157-169. doi:10.1113/EP086534

Vignoli, B., Battistini, G., Melani, R., Blum, R., Santi, S., Berardi, N. and Canossa, M. (2016). Peri-synaptic glia recycles brain-derived neurotrophic factor for LTP stabilization and memory retention. *Neuron* **92**, 873-887. doi:10.1016/j.neuron.2016.09.031

Wu, V. W., Nishiyama, N. and Schwartz, J. P. (1998). A culture model of reactive astrocytes: increased nerve growth factor synthesis and reexpression of cytokine responsiveness. *J. Neurochem.* **71**, 749-756. doi:10.1046/j.1471-4159.1998.71020749.x

Yang, L., Zhang, W., Peng, J. and Yin, F. (2018). Heterozygous KIDINS220 mutation leads to spastic paraplegia and obesity in an Asian girl. *Eur. J. Neurol.* **25**, e53-e54. doi:10.1111/ene.13600

Yanpallewar, S., Fulgenzi, G., Tomassoni-Ardori, F., Barrick, C. and Tessarollo, L. (2021). Delayed onset of inherited ALS by deletion of the BDNF receptor TrkB.T1 is non-cell autonomous. *Exp. Neurol.* **337**, 113576. doi:10.1016/j.expneurol.2020.113576

Zafra, F., Lindholm, D., Castren, E., Hartikka, J. and Thoenen, H. (1992). Regulation of brain-derived neurotrophic factor and nerve growth factor mRNA in primary cultures of hippocampal neurons and astrocytes. *J. Neurosci.* **12**, 4793-4799. doi:10.1523/JNEUROSCI.12-12-04793.1992

Zhao, M., Chen, Y.-J., Wang, M.-W., Lin, X.-H., Dong, E.-L., Chen, W.-J., Wang, N. and Lin, X. (2019). Genetic and clinical profile of chinese patients with autosomal dominant spastic paraplegia. *Mol. Diagn. Ther.* **23**, 781-789. doi:10.1007/s40291-019-00426-w

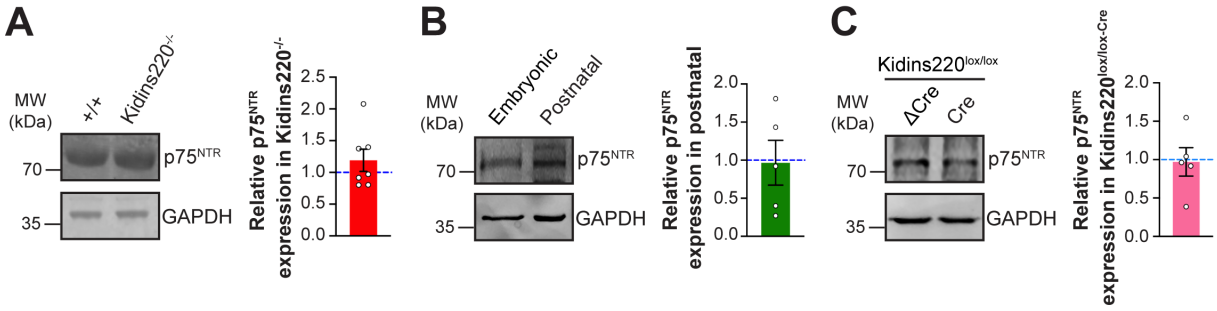

Fig. 1. $p75^{NTR}$ expression levels are not different in embryonic and postnatal cells and do not depend on Kidins220.

Protein extracts from embryonic wild type and Kidins220$^{-/-}$ astrocytes (**A**), from wild type embryonic and postnatal astrocytes (**B**) and from Kidins220$^{lox/lox\text{-}\Delta Cre}$ and Kidins220$^{lox/lox\text{-}Cre}$ astrocytes (**C**) were analyzed by western blotting with anti-$p75^{NTR}$ antibodies. Representative immunoblots are shown on the left; quantification of immunoreactive bands is on the right. The intensity of bands from Kidins220$^{-/-}$, postnatal and Kidins220$^{lox/lox\text{-}Cre}$ samples were normalized to the corresponding control samples within the same nitrocellulose membrane. $p>0.05$, one sample Student's *t*-test, n=7 independent cultures of both genotypes in (A), n=5 in (B) and (C).

Journal of Cell Science • Supplementary information

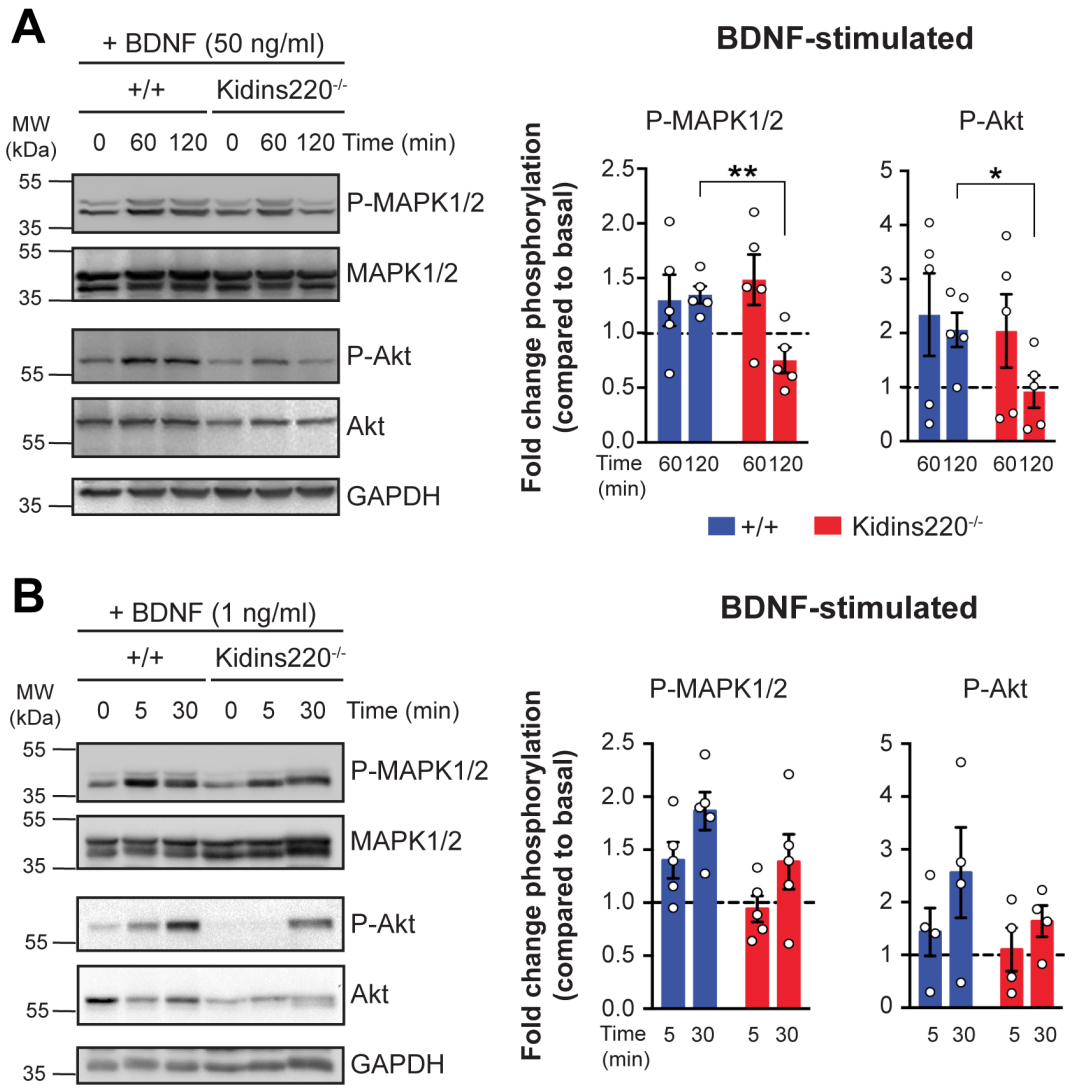

Fig. 2. Activation of signaling pathways upon administration of 1 ng/ml BDNF in embryonic astrocytes.

(**A**) Wild type and Kidins220$^{-/-}$ embryonic astrocyte cultures were treated with 50 ng/ml BDNF for 60 min and 120 min or left untreated (time 0). (**B**) Wild type and Kidins220$^{-/-}$ embryonic astrocyte cultures were treated with 1 ng/ml BDNF for 5 and 30 min or left untreated (time 0). In both (A) and (B), lysates were analyzed for phosphorylated MAPK1/2 (Thr202/Tyr204) and Akt (Ser473). PLCγ did not show any reliable activation at 1 ng/ml BDNF concentration (not shown). Membranes were subsequently stripped and re-probed for the total amount of the same protein. *Left*: Representative immunoblots. *Right*: Time dependence of MAPK1/2 and Akt phosphorylation upon BDNF stimulation in wild type and Kidins220$^{-/-}$ astrocytes. The graphs express the fold change activation of MAPK1/2 and Akt compared to the untreated phosphorylation levels for each genotype, set to

Journal of Cell Science • Supplementary information

1 (dashed line in all graphs). For further details, see legend to Fig. 1 and Methods. For MAPK, we report the sum of MAPK1 and MAPK2 immunoreactivity. *p<0.05, **p<0.01, unpaired Student's *t*-test, n=5 in (A) n=4-5 in (B) for both wild type and Kidins220$^{-/-}$ cultures. Values are expressed as means ± S.E.M.

Journal of Cell Science • Supplementary information

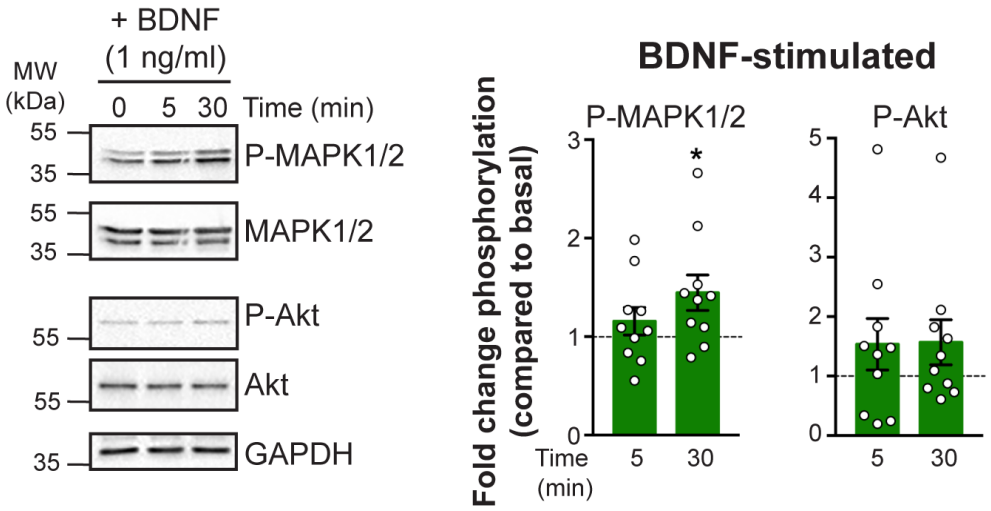

Fig. S3. Activation of signaling pathways upon administration of 1 ng/ml BDNF in wild type postnatal astrocytes.

Experiments as in Suppl. Figure 1, but for wild type postnatal astrocytes cultures. *p<0.05, one sample Student's *t*-test compared to baseline, n=10 independent cultures. Values are expressed as means ± S.E.M.

Journal of Cell Science • Supplementary information

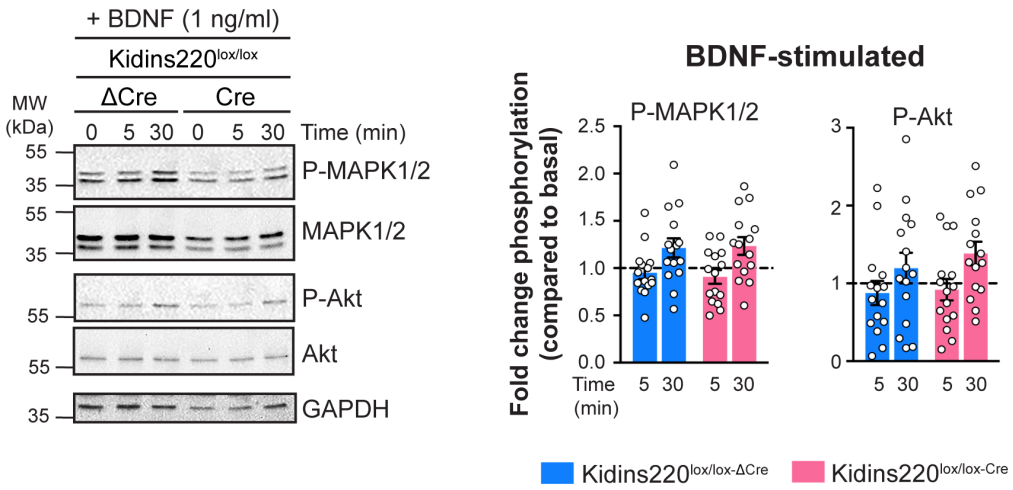

Fig. S4. Activation of signaling pathways upon administration of 1 ng/ml BDNF in Kidins220-deficient postnatal astrocytes.

Experiments as in Suppl. Figure 2, but for Kidins220$^{lox/lox\text{-}Cre}$ and Kidins220$^{lox/lox\text{-}\Delta Cre}$ astrocytes cultures. $p>0.05$, unpaired Student's *t*-test, n=15 independent cultures. In all experiments, GAPDH was used as a loading control. Values are expressed as means ± S.E.M.

Journal of Cell Science • Supplementary information

Table S1. List of primers used for the RT-qPCR analysis.

Gene	GenBank Accession	Forward primer (5' → 3')	Reverse primer (5' → 3')
Slc1a2 (GLT-1)	NM_001077514.4	ACTGGCTGCTGGATAGAATGA	AATGGTGTCCAGCTCAGACT
Kcnj10 (Kir4.1)	NM_001039484.1	GCCCCGCGATTTATCAGAG	TCCATTCTCACATTGCTCCG
Aqp4	NM_009700.3	CTGTGGCAGCGAGATAATGG	GCCTTTCTGGGAACTCACAC
Gja1 (Cnx43)	NM_010288.3	CTTTGACTTCAGCCTCCAAGG	GGGCACCTCTCTTTCACTTAAT
Housekeeping genes			
TBP	NM_013684.3	ACTTCGTGCAAGAAATGCTGAAT	CAGTTGTCCGTGGCTCTCTTATT
TRFR	NM_011638.4	AGACCTTGCACTGTTTGGACATG	GGTGTGTATGGATCACCAGTTCCTA
TUBB2	NM_009450.2	CAAGGCTTTCCTGCACTGGT	AACTCCATCTCGTCCATGCC

Journal of Cell Science • Supplementary information